Proton spin at small x

YURI KOVCHEGOV
THE OHIO STATE UNIVERSITY

Credits

- Based on work done with Dan Pitonyak and Matt Sievert (2015-2018, 2021-present), Florian Cougoulic (2019-present), Gabe Santiago (2020-present), Josh Tawabutr (2020-present), Andrey Tarasov (2021-present), Daniel Adamiak, Wally Melnitchouk, Nobuo Sato (2021-present), Jeremy Borden (2023-present), Ming Li (2023-present), Brandon Manley (2023-present), Nick Baldonado (2022-present), Zardo Becker (2024-present).

Outline

- Introduction to the proton spin puzzle
- Quark and gluon helicity evolution at small x:
  - Dipole picture of high-energy scattering
  - Sub-eikonal operators
  - Quark and gluon helicity distributions at small x & polarized dipoles
  - Small-x evolution equations for quark and gluon helicity
  - Solution of helicity evolution equations and the small-x asymptotics of quark and gluon helicity distributions
  - Phenomenology: first fit of small-x polarized DIS+SIDIS+pp data using evolution in x
- Orbital angular momentum (OAM) distributions at small x:
  - OAM distributions at small x
  - Small-x evolution for OAM distributions
  - Measuring OAM at small x at EIC
- Conclusions

Proton Spin Puzzle:
an Introduction

Proton Spin

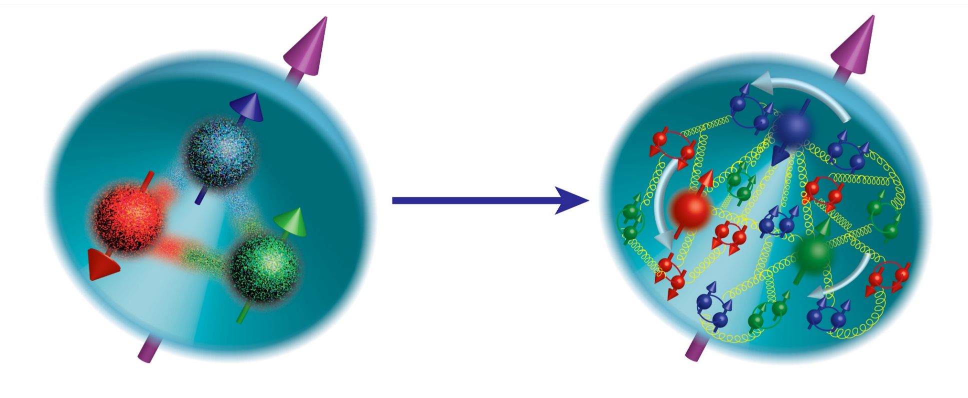

Our understanding of nucleon spin structure has evolved:

- In the 1980's the proton spin was thought of as a sum of constituent quark spins (left panel)

- Currently we believe that the proton spin is a sum of the spins of valence and sea quarks and of gluons, along with the orbital angular momenta of quarks and gluons (right panel)

Helicity Distributions

- To quantify the contributions of quarks and gluons to the proton spin on defines helicity distribution functions: number of quarks/gluons with spin parallel to the proton momentum minus the number of quarks/gluons with the spin opposite to the proton momentum:

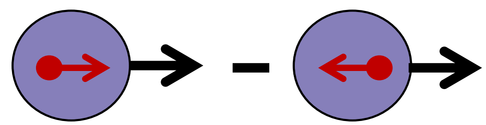

- The helicity parton distributions are

$$\Delta f(x, Q^2) \equiv f^+(x, Q^2) - f^-(x, Q^2)$$

with the flavor-singlet quark helicity distribution

$$\Delta\Sigma \equiv \Delta u + \Delta\bar{u} + \Delta d + \Delta\bar{d} + \Delta s + \Delta\bar{s}$$

and $\Delta G(x, Q^2)$ the gluon helicity distribution.

Proton Helicity Sum Rule

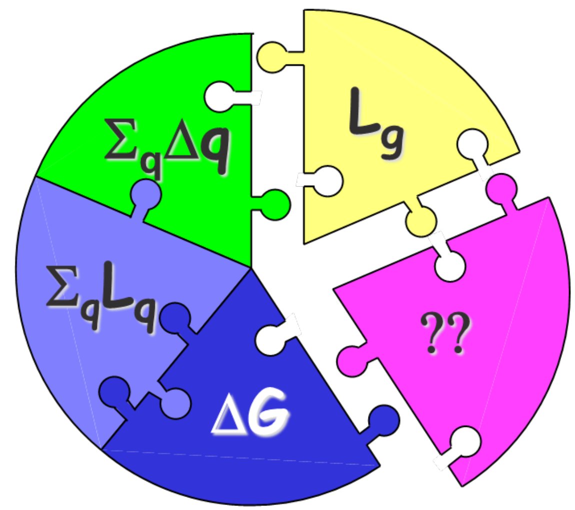

- Helicity sum rule (Jaffe&Manohar, 1989; cf. Ji, 1997):

$$\frac{1}{2} = S_q + L_q + S_g + L_g$$

with the net quark and gluon spin

$$S_q(Q^2) = \frac{1}{2} \int_0^1 dx \, \Delta\Sigma(x, Q^2) \qquad S_g(Q^2) = \int_0^1 dx \, \Delta G(x, Q^2)$$

- L_q and L_g are the quark and gluon orbital angular momenta (OAM)

Proton Spin Puzzle

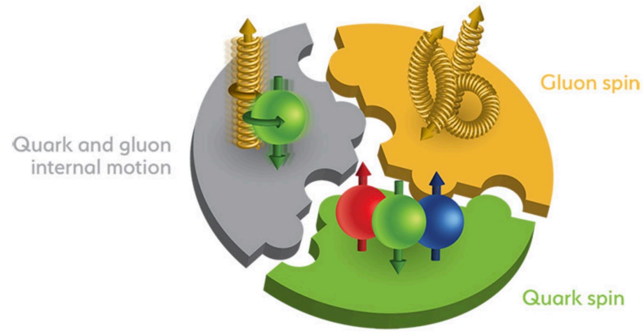

- The spin puzzle began when the EMC collaboration measured the proton g_1 structure function ca 1988. Their data resulted in

$$S_q \approx 0.03$$

- It appeared (constituent) quarks do not carry all of the proton spin (which would have naively corresponded to $S_q = 1/2$).

$$\frac{1}{2} = S_q + L_q + S_g + L_g$$

- Missing spin can be
  - Carried by gluons
  - In the orbital angular momenta of quarks and gluons
  - At small x:

$$S_q(Q^2) = \frac{1}{2} \int_0^1 dx \, \Delta\Sigma(x, Q^2) \qquad S_g(Q^2) = \int_0^1 dx \, \Delta G(x, Q^2)$$

Can't integrate down to zero, use x_{min} instead!

  - Or all of the above!

Current Knowledge of Proton Spin

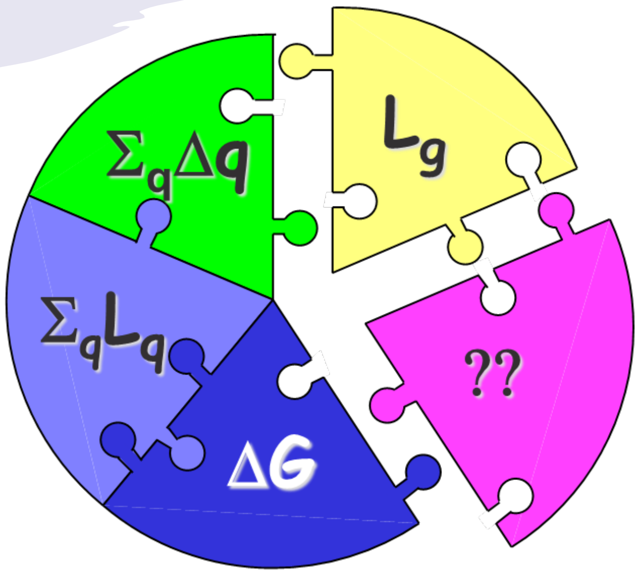

- The proton spin carried by the quarks is estimated to be (for $0.001 < x < 1$)

$$S_q(Q^2 = 10 \text{ GeV}^2) \in [0.15, 0.2]$$

- The proton spin carried by the gluons is (for $0.01 < x < 1$, STAR+PHENIX+COMPASS +HERMES+… , analyzed by DSSV, JAM, NNPDF…)

$$S_G(Q^2 = 10 \text{ GeV}^2) \in [0.13, 0.26]$$

- Negative S_G is also possible (JAM '22), but not likely.
- Unfortunately, the uncertainties are large. Note also that the x-ranges are limited, with more spin (positive or negative) possible at small x.

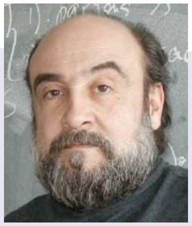

The DGLAP Equation

The Dokshitzer-Gribov-Lipatov-Altarelli-Parisi (DGLAP) evolution equation is a renormalization group equation describing variation of parton distributions with Q^2. Diagrammatically we can represent it as follows:

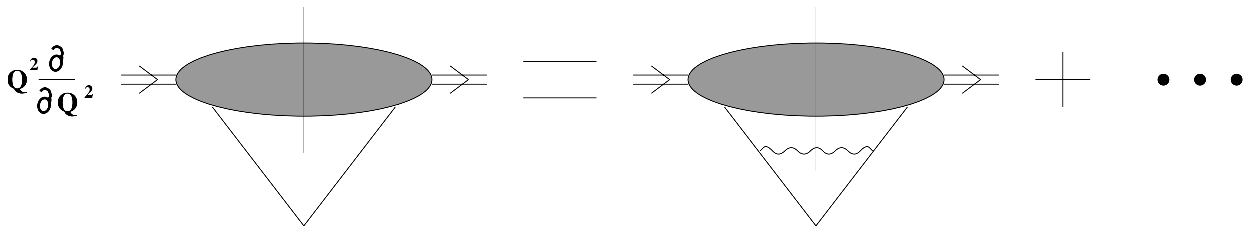

- For the helicity-dependent case the equations read

$$Q^2 \frac{\partial}{\partial Q^2} \begin{pmatrix} \Delta\Sigma(x,Q^2) \\ \Delta G(x,Q^2) \end{pmatrix} = \frac{\alpha_s(Q^2)}{2\pi} \int_x^1 \frac{dz}{z} \begin{pmatrix} \Delta P_{qq}(z) & \Delta P_{qG}(z) \\ \Delta P_{Gq}(z) & \Delta P_{GG}(z) \end{pmatrix} \begin{pmatrix} \Delta\Sigma(\frac{x}{z},Q^2) \\ \Delta G(\frac{x}{z},Q^2) \end{pmatrix}$$

(ΔP_{ij} are the spin-dependent splitting functions).

DGLAP Evolution: the Physical Meaning

As we increase the resolution (decrease 1/Q),
we "see" more partons:

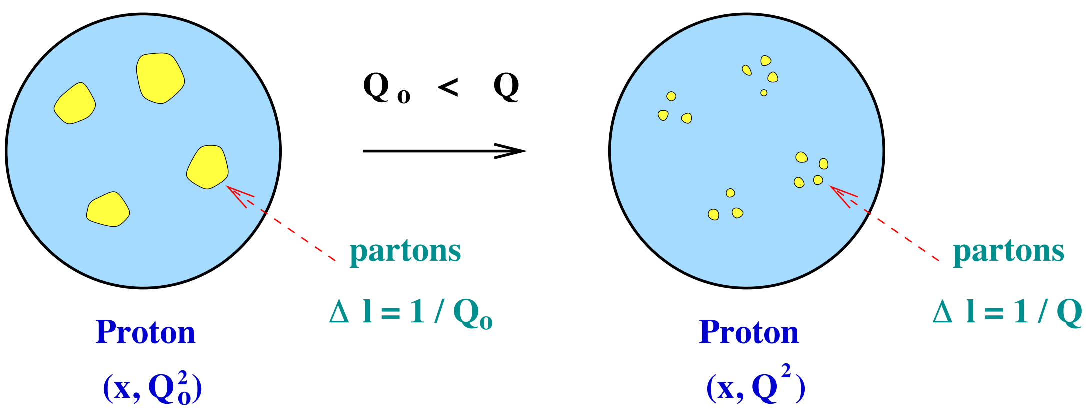

Indeed, this RG flow is on the cover of Peskin& Schroeder:

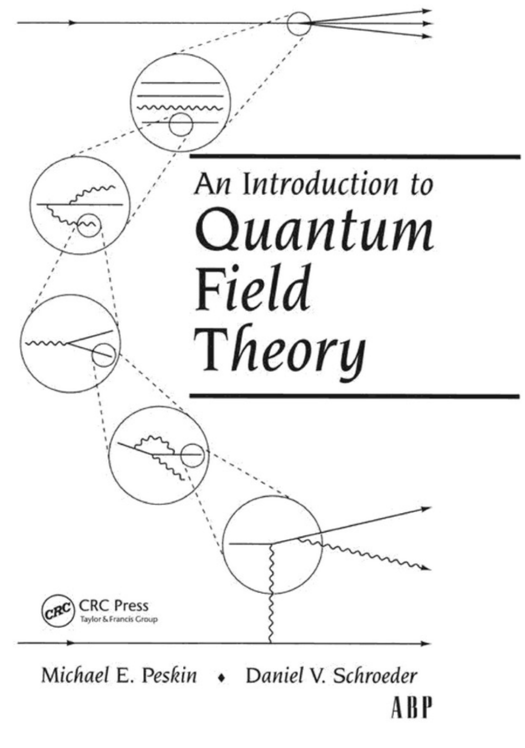

How DGLAP works

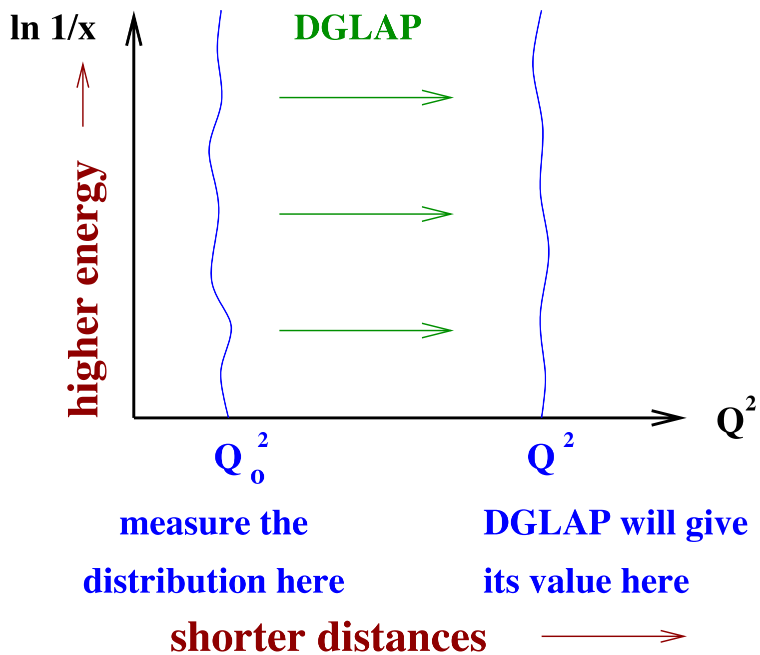

- One still needs to measure the PDFs at the initial scale Q_0^2 (at all values of x). Then the DGLAP equation would predict the PDFs at higher Q^2.
- In practice one parametrizes the x-dependence of PDFs at Q_0^2 and varies the parameters until they fit the data at all available Q^2.
- Problem/feature: DGLAP equation does not quite predict the x-dependence of PDFs. The x-dependence is strongly affected by the initial conditions at Q_0^2.
- Consequence: DGLAP **cannot predict** how much spin there is at small x!

Gluons and Quarks at Small-x

- There is a large number of small-x gluons (and sea quarks) in a proton:

x (# gluons or quarks)

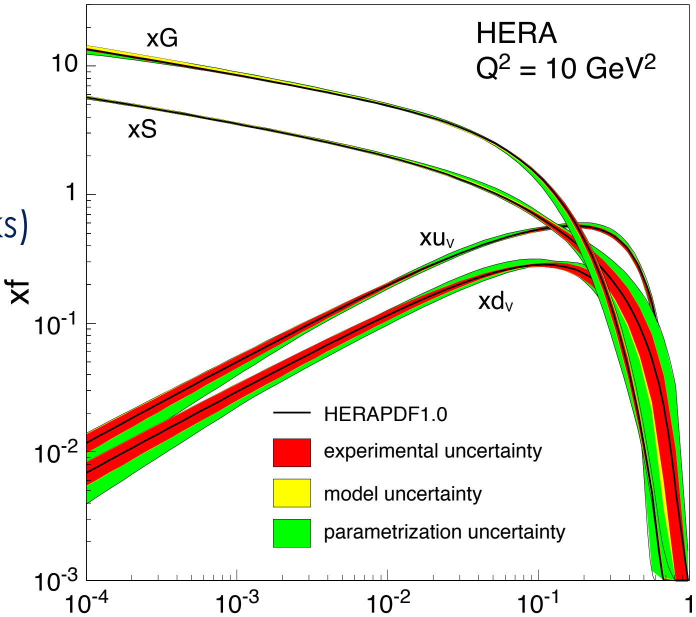

x =fraction of the proton momentum they carry

Can the small-x gluons and quarks carry a lot of the proton spin?

- $G(x, Q^2)$, $q(x, Q^2)$ = gluon and quark number densities / parton distribution functions (q=u,d, or S for sea).

How much spin is there at small x?

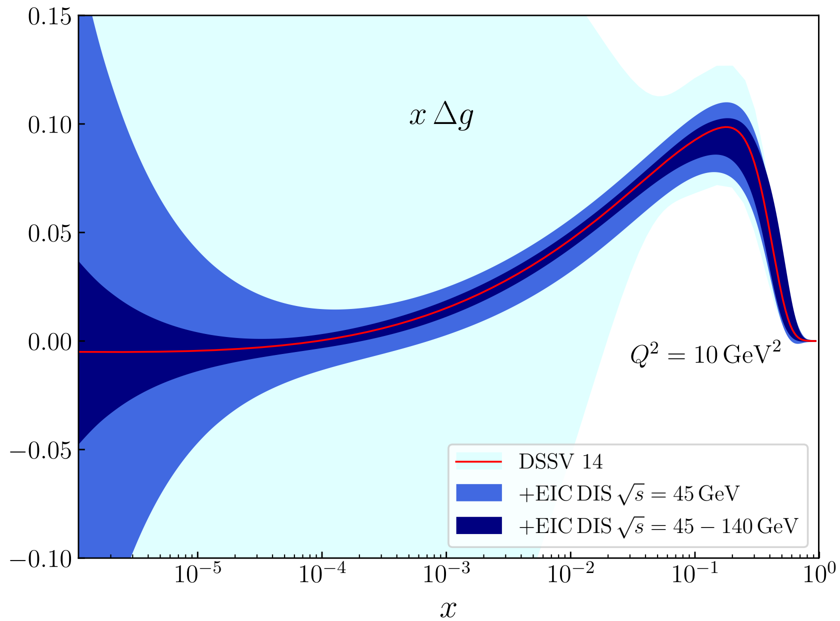

- E. Aschenauer et al, 2020 (DGLAP-based helicity PDF extraction from data)
- Uncertainties are very large at small x. Note that this is xΔG, the uncertainties for ΔG are 1/x = 100-10000 times larger! EIC will reduce them, but only where there will be data.

$$\frac{1}{2} = S_q + L_q + S_g + L_g$$

Small-x Spin Challenge

- Can we constrain theoretically the amount of proton spin and OAM coming from small x?

- Any existing and future experiment probes the helicity distributions and OAM down to some x_{min} .

$$S_q(Q^2) = \frac{1}{2} \int\limits_0^1 dx\, \Delta\Sigma(x, Q^2) \qquad S_g(Q^2) = \int\limits_0^1 dx\, \Delta G(x, Q^2)$$

$$L_{q+\bar{q}}(Q^2) = \int\limits_0^1 dx\, L_{q+\bar{q}}(x, Q^2) \qquad L_G(Q^2) = \int\limits_0^1 dx\, L_G(x, Q^2)$$

- At very small x (for the proton), saturation sets in: that region likely carries a negligible amount of proton spin. But what happens at larger (but still small) x?

Philosophy of small-x approach to spin

- DGLAP equation evolves in Q^2, it does not evolve in x.
- Hence, DGLAP-based analyses (DSSV, NNPDF, standard JAM) cannot predict the x-dependence of PDFs.
- If we want to predict helicity PDFs at small x, we need a different evolution equation that evolves in x.
- Such equations were constructed by D. Pitonyak, M. Sievert, and YK, (KPS, 2015-2018) along with a recent important correction by F. Cougoulic, YK, A. Tarasov, Y. Tawabutr (KPS-CTT) in 2022 + another one by J. Borden, YK, M. Li 2024 & G. Chirilli (2021) (KPS-CTT-BCL); both works use an approach similar to the BK/JIMWLK evolution.
- Other important work on spin at small x: J. Bartels, B. Ermolaev, M. Ryskin '95-'96; Y. Hatta et al '16; R. Boussarie, Y. Hatta, F. Yuan '19. Significant related works by R. Kirschner and L. Lipatov '83; T. Altinoluk, G. Beuf et al '20, '21.


The BFKL Equation


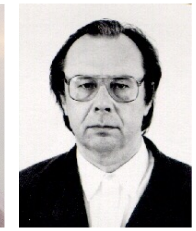

Balitsky, Fadin, Kuraev, Lipatov '78

Start with N gluons in the proton's wave function. As we increase the energy a new gluon can be emitted by either one of the N gluons. The number of newly emitted particles is proportional to N.

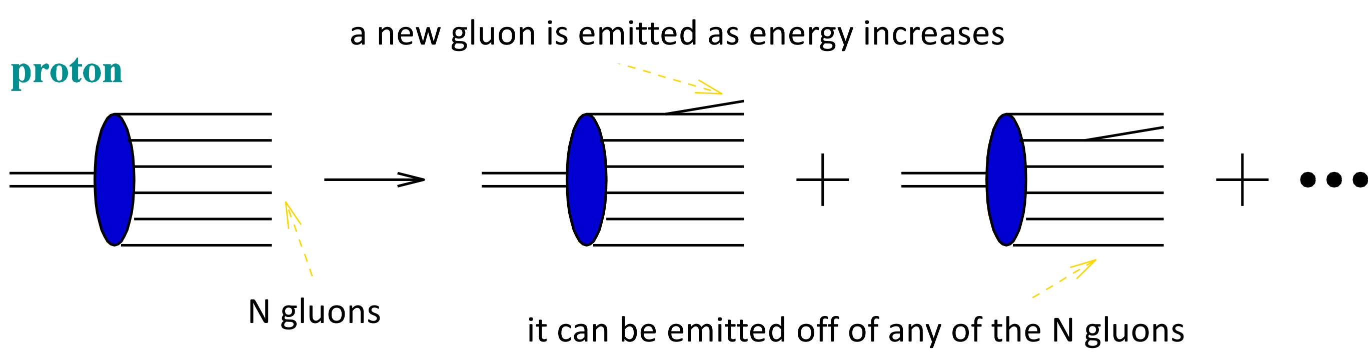

The BFKL equation for the number of gluons N reads:

$$\frac{\partial}{\partial \ln(1/x)} N(x,Q^2) = \alpha_S K_{BFKL} \otimes N(x,Q^2)$$

Helicity Evolution at Small x

- To understand how much of the proton's spin is at small x one can construct a helicity analogue of the BFKL equation:

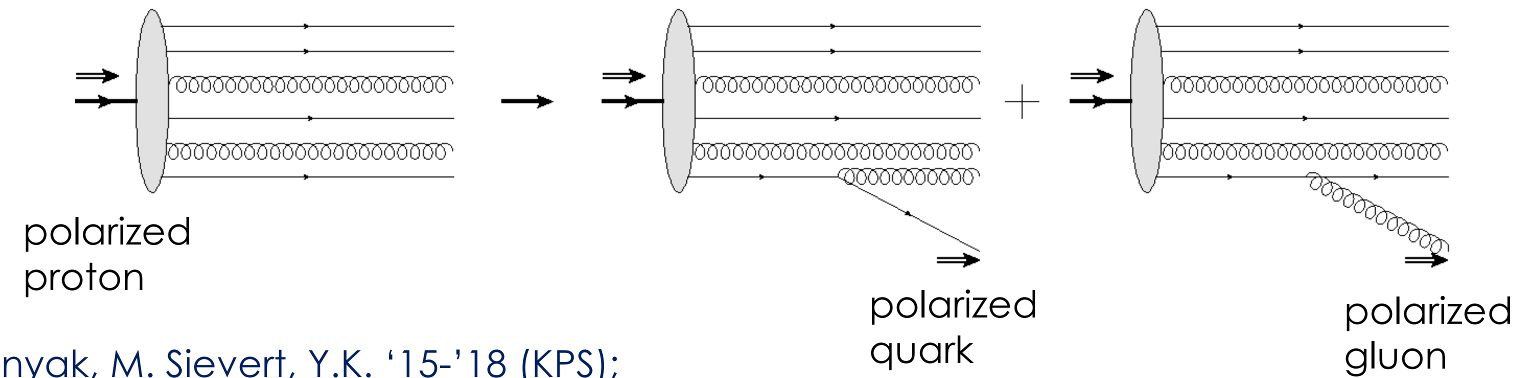

D. Pitonyak, M. Sievert, Y.K. '15-'18 (KPS);
F. Cougoulic, YK, A. Tarasov, Y. Tawabutr '22;
J. Borden, YK, M. Li '24; G. Chirilli '21.

- These new helicity evolution equations are subtle, since they must keep track of both quark and gluon helicities. (Other small-x evolution equations, BFKL/BK/JIMWLK, only have gluons at leading order.)

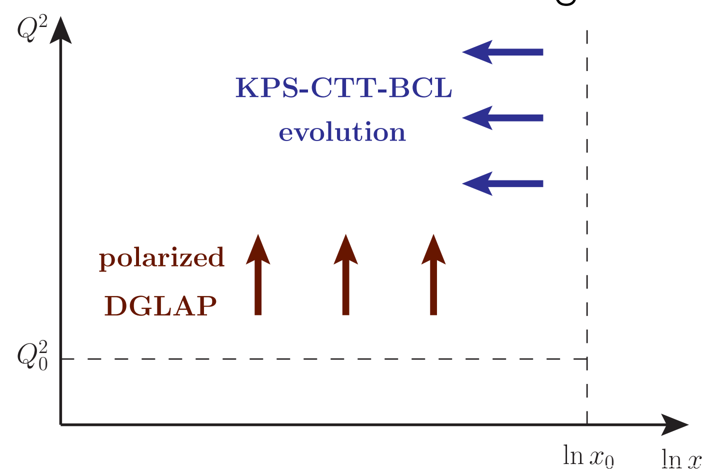

EIC & Spin Puzzle

Still, even with the EIC data we need to extrapolate quark and gluon spin down to smaller x.

- Parton helicity distributions are sensitive to low-x physics.
- EIC would have an unprecedented low-x reach for a polarized DIS experiment, allowing to pinpoint the values of quark and gluon contributions to proton's spin (EIC WP '12):

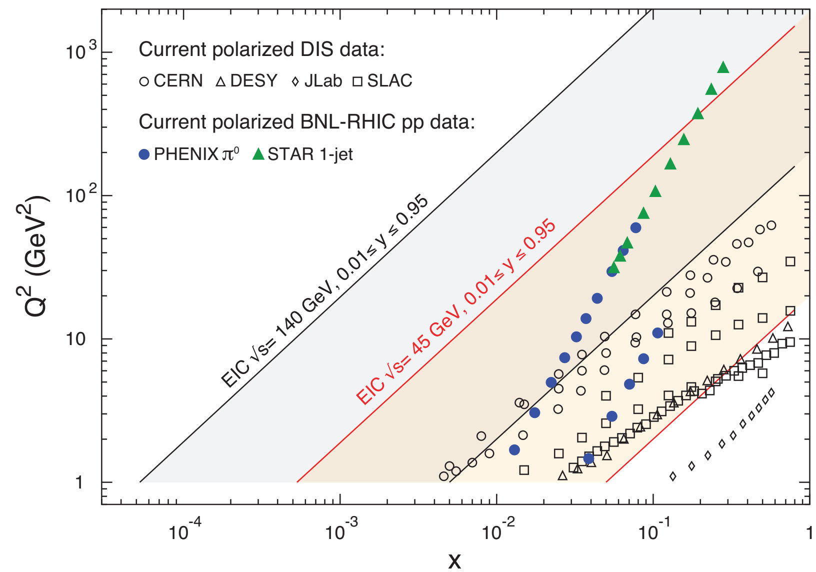

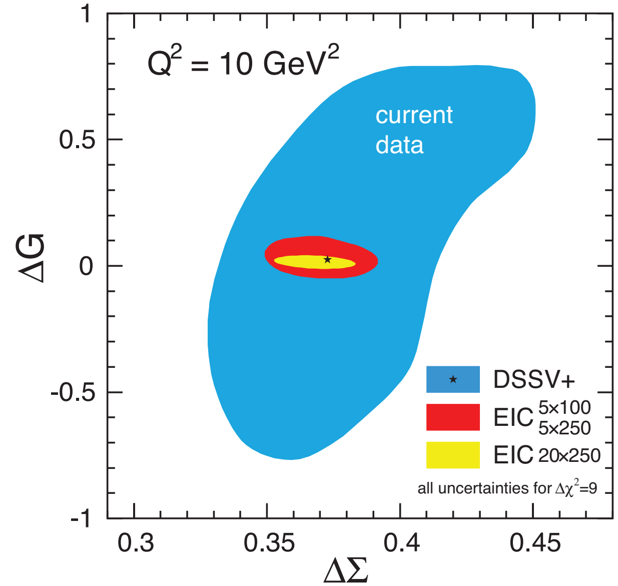

- ΔG and ΔΣ are integrated over x in the 0.001 < x < 1 interval.

Quark and Gluon Helicity at Small x

YK, D. Pitonyak, M. Sievert, arXiv:1511.06737 [hep-ph], arXiv:1610.06197 [hep-ph] (KPS);
YK, M. Sievert, arXiv:1505.01176 [hep-ph], arXiv:1808.09010 [hep-ph];
F. Cougoulic, YK, A. Tarasov, and Y. Tawabutr, arXiv:2204.11898 [hep-ph] (KPS-CTT);
J. Borden, YK, M. Li, 2406.11647 [hep-ph]; G. Chirilli, 2101.12744 [hep-ph] (KPS-CTT-BCL).

Dipole picture of high-energy scattering

Dipole picture of DIS

$$W^{\mu\nu} = \frac{1}{4\pi M_p} \int d^4x \, e^{iq\cdot x} \langle P | j^\mu(x) \, j^\nu(0) | P \rangle$$

$$q^\mu = \left(\frac{Q^2}{2q^-}, q^-, 0_\perp \right)$$

Large q^- → large x^- separation

$$e^{iq\cdot x} = e^{i\frac{Q^2}{2q^-}x^- + iq^- x^+}$$

$$x^\pm = \frac{t \pm z}{\sqrt{2}}$$

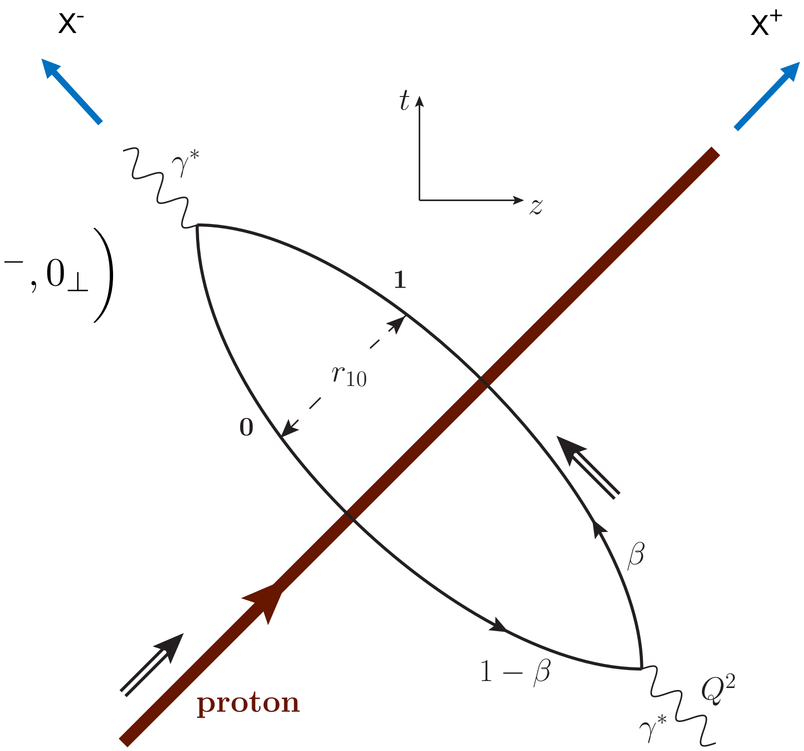

aka the “shock wave”

Dipole picture of DIS

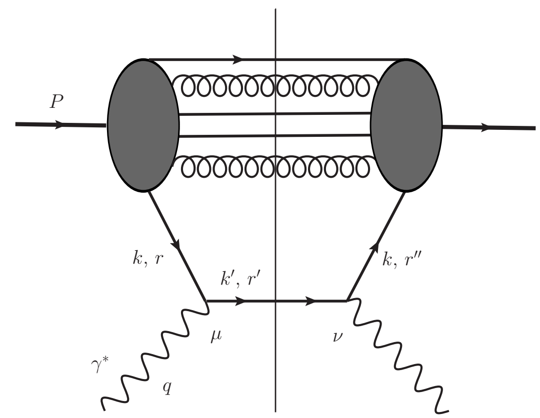

- At small x, the dominant contribution to DIS structure functions does not come from the handbag diagram.

- Instead, the dominant terms comes from the dipole picture of DIS, where the virtual photon splits into a quark-antiquark pair, which then interacts with the target.

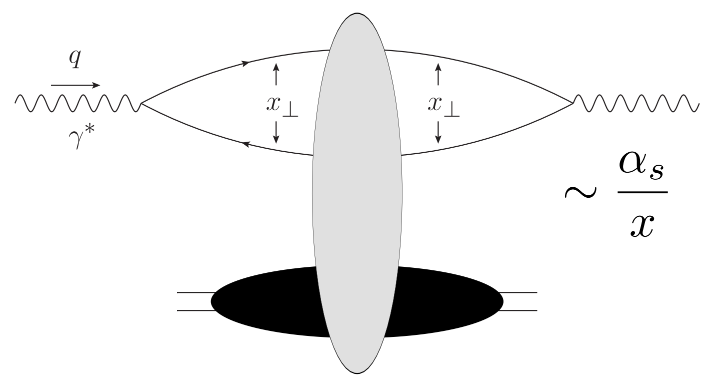

$$\sim \frac{\alpha_s}{x}$$

Dipole Amplitude

- The total DIS cross section is expressed in terms of the (Im part of the) forward quark dipole amplitude N:

$$\sigma_{tot}^{\gamma^* A} = \int \frac{d^2 x_\perp}{2\,\pi}\, d^2 b_\perp \int\limits_0^1 \frac{dz}{z\,(1-z)}\, |\Psi^{\gamma^* \to q\bar{q}}(\vec{x}_\perp, z)|^2 \; N(\vec{x}_\perp, \vec{b}_\perp, Y)$$

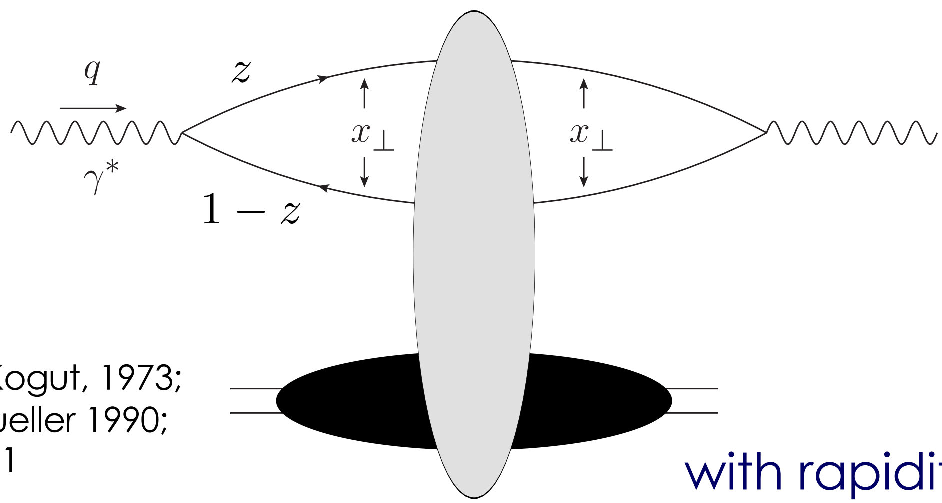

b is the Fourier conjugate to q with t = - q^2, making the dipole amplitude N similar to the GPDs at zero skewness.

$b_\perp, \; Y$

Gribov, 1970; Bjorken and Kogut, 1973; Frankfurt, Strikman 1988; Mueller 1990; Nikolaev and Zakharov 1991

with rapidity Y=ln(1/x)

Dipole Amplitude

- The quark dipole amplitude is defined by

$$N(\underline{x}_1, \underline{x}_2) = 1 - \frac{1}{N_c} \left\langle \mathrm{tr} \left[V(\underline{x}_1) \, V^\dagger(\underline{x}_2) \right] \right\rangle$$

- Here we use the Wilson lines along the light-cone direction

$$V_{\underline{x}} = \mathcal{P} \exp \left[ig \int\limits_{-\infty}^{\infty} dx^- A^+(0^+, x^-, \underline{x}) \right]$$

- In the classical Glauber-Mueller/McLerran-Venugopalan approach the dipole amplitude resums multiple rescatterings:

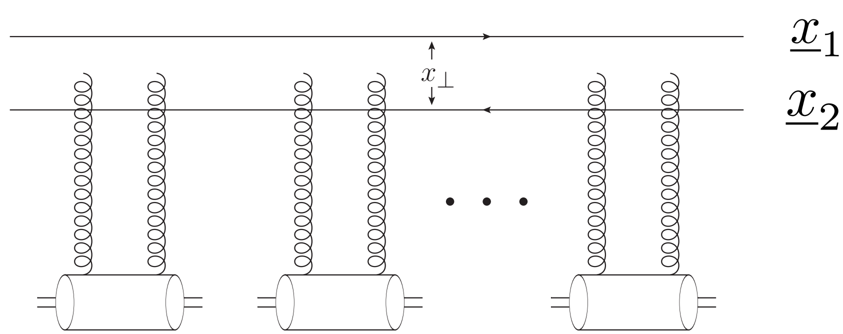

Small-x Evolution

- Energy dependence comes in through the long-lived *s*-channel gluon corrections (higher Fock states):

$$\alpha_s \, \ln s \sim \alpha_s \, \ln \frac{1}{x} \sim 1$$

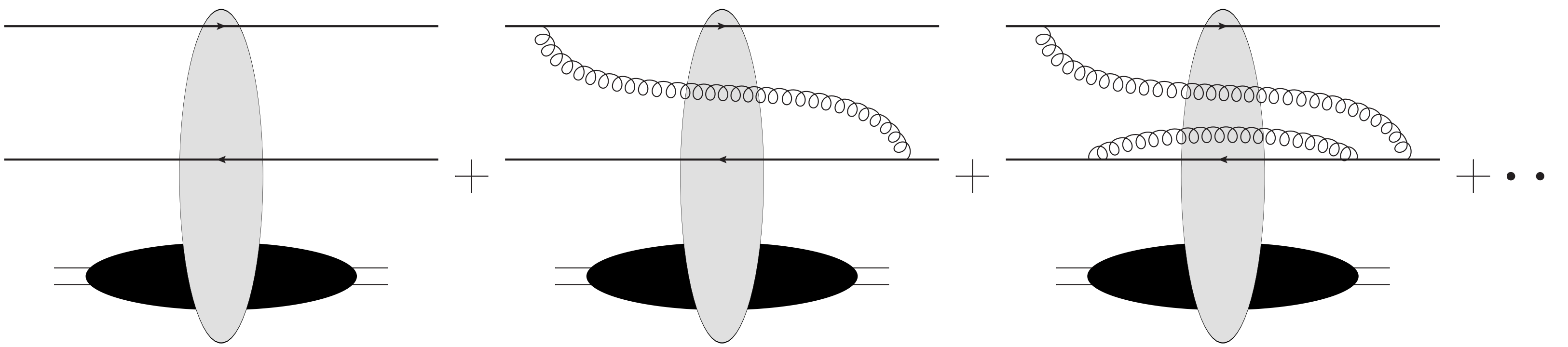

These extra gluons bring in powers of α_S ln s, such that when $\alpha_S << 1$ and ln s >>1 this parameter is $\alpha_S \ln s \sim 1$ (leading logarithmic approximation, LLA).

Small-x Evolution: Large N_c Limit

- How do we resum this cascade of gluons?
- The simplification comes from the large-Nc limit, where each gluon becomes a quark-antiquark pair:

$$3 \otimes \bar{3} = 1 \oplus 8 \quad \Rightarrow \quad N_c \otimes \bar{N}_c = 1 \oplus (N_c^2 - 1) \approx N_c^2 - 1$$

- Gluon cascade becomes a dipole cascade (each color outlines a dipole):

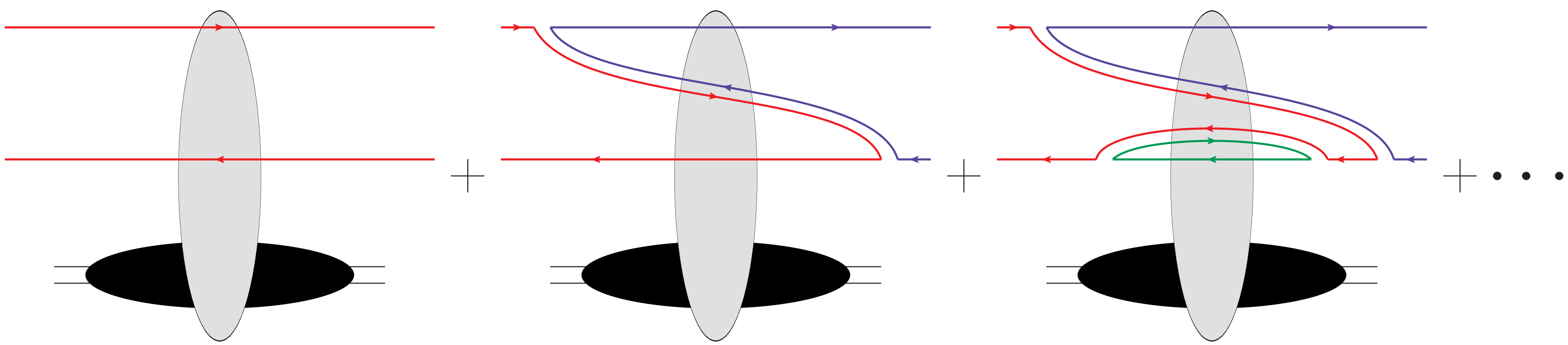

Mueller's Dipole Model

To include the quantum evolution in a dipole amplitude one Can use the approach developed by A. H. Mueller in '93-'94. The goal is to resum leading logs of energy, α log s, just like for the BFKL equation.

Emission of a small-x gluon taken in the large-N_C limit would split the original color dipole in two:

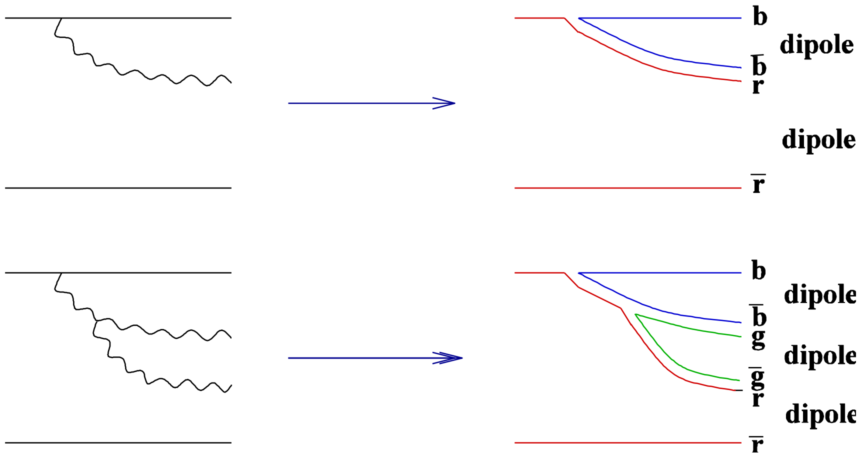

$$3 \otimes \bar{3} = 1 \oplus 8 \quad \Rightarrow \quad N_c \otimes \bar{N}_c = 1 \oplus (N_c^2 - 1) \approx N_c^2 - 1$$

Notation (Large-N_c)

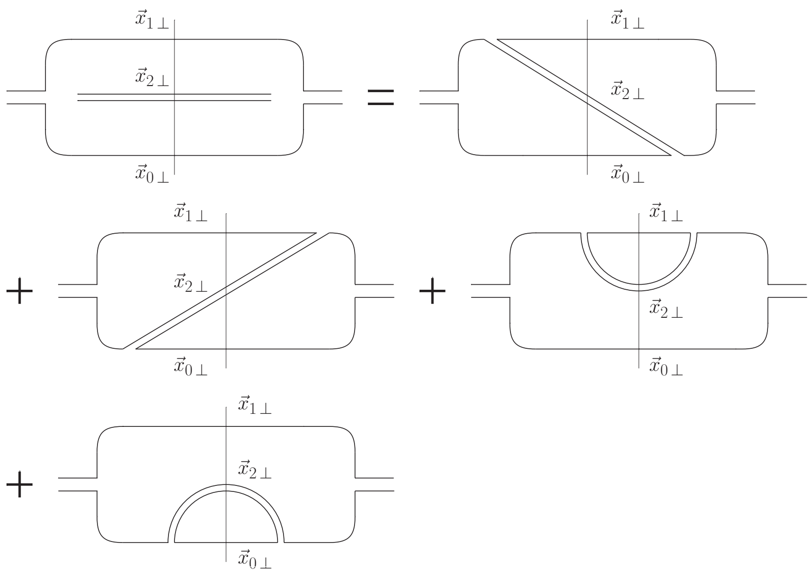

Real emissions in the amplitude squared

(dashed line – all Glauber-Mueller exchanges at light-cone time =0)

Virtual corrections in the amplitude (wave function)

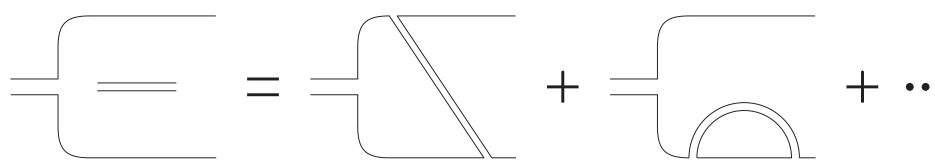

Nonlinear Evolution

To sum up the gluon cascade at large-N_C we write the following equation for the dipole S-matrix:

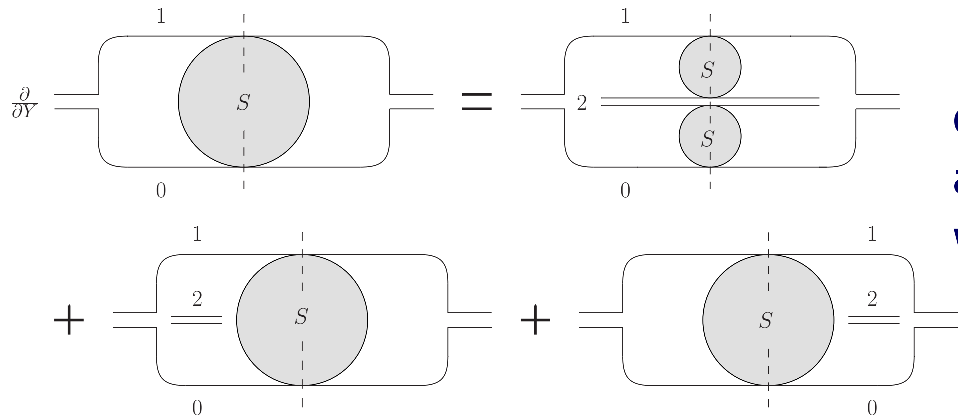

dashed line = all interactions with the target

$$Y = \ln \frac{1}{x} \sim \ln s$$

$$\partial_Y S_{\mathbf{x}_0,\mathbf{x}_1}(Y) = \frac{\alpha_s N_c}{2\pi^2} \int d^2 x_2 \frac{x_{01}^2}{x_{02}^2 \, x_{21}^2} \left[S_{\mathbf{x}_0,\mathbf{x}_2}(Y) \, S_{\mathbf{x}_2,\mathbf{x}_1}(Y) - S_{\mathbf{x}_0,\mathbf{x}_1}(Y) \right]$$

Remembering that S=1 + i T = 1 - N where N = Im(T) we can rewrite this equation in terms of the dipole scattering amplitude N.

Nonlinear evolution at large N_c

As N=1-S we write

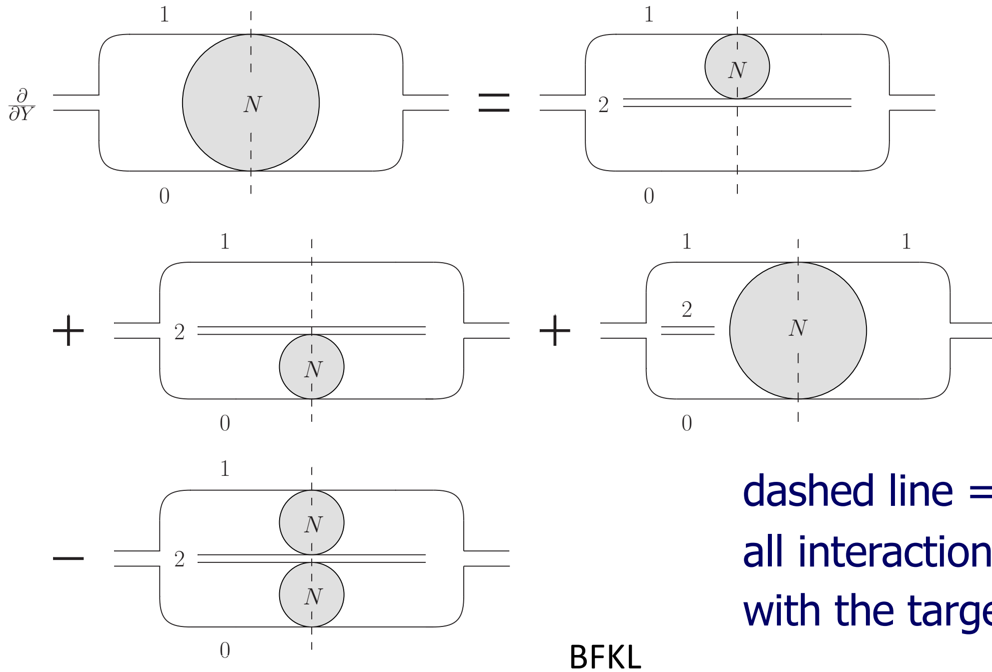

BFKL

$$\partial_Y N_{\mathbf{x}_0,\mathbf{x}_1}(Y) = \frac{\alpha_s N_c}{2\pi^2} \int d^2 x_2 \, \frac{x_{01}^2}{x_{02}^2 \, x_{21}^2} \, [N_{\mathbf{x}_0,\mathbf{x}_2}(Y) + N_{\mathbf{x}_2,\mathbf{x}_1}(Y) - N_{\mathbf{x}_0,\mathbf{x}_1}(Y) - N_{\mathbf{x}_0,\mathbf{x}_2}(Y)\, N_{\mathbf{x}_2,\mathbf{x}_1}(Y)]$$

Balitsky '96, Yu.K. '99; beyond large N_c, JIMWLK evolution, 0.1% correction for the dipole amplitude

Re-summing gluon cascade

- At large N_c the gluon cascade turns into a dipole cascade. We are resumming the dipole cascade, with each dipole interacting with the target independently:

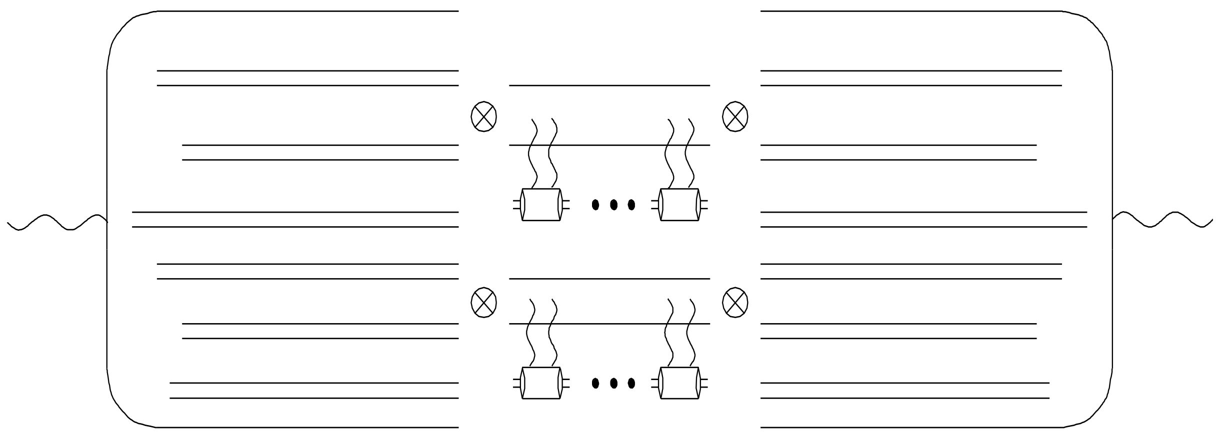

JIMWLK: derivation outline

- As a test operator, take a pair of Wilson lines (not a dipole!):

$$\hat{O}_{\vec{x}_{1\perp},\vec{x}_{0\perp}} = V_{\vec{x}_{1\perp}} \otimes V^{\dagger}_{\vec{x}_{0\perp}}$$

- Construct the evolution of this operator by summing the following familiar diagrams:

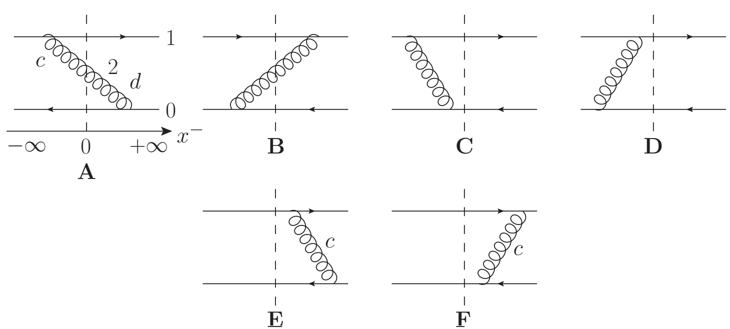

real

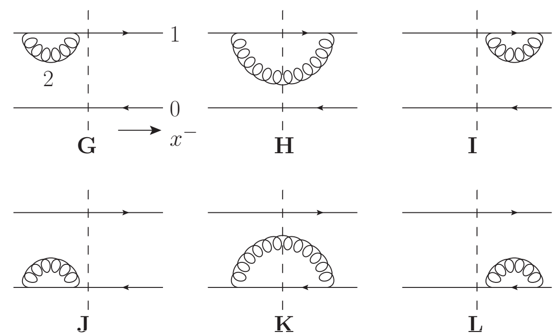

virtual

The JIMWLK Equation

- In the end one arrive at the JIMWLK evolution equation (Jalilian-Marian—Iancu–McLerran—Weigert—Leonidov—Kovner, 1997-2002):

$$\partial_Y W_Y[\alpha] = \alpha_s \left\{ \frac{1}{2} \int d^2x_\perp \, d^2y_\perp \, \frac{\delta^2}{\delta\alpha^a(x^-, \vec{x}_\perp) \, \delta\alpha^b(y^-, \vec{y}_\perp)} \left[\eta^{ab}_{\vec{x}_\perp \vec{y}_\perp} W_Y[\alpha] \right] - \int d^2x_\perp \, \frac{\delta}{\delta\alpha^a(x^-, \vec{x}_\perp)} \left[\nu^a_{\vec{x}_\perp} W_Y[\alpha] \right] \right\}$$

with

$$\eta^{ab}_{\vec{x}_{1\perp} \vec{x}_{0\perp}} = \frac{4}{g^2 \, \pi^2} \int d^2x_2 \, \frac{\vec{x}_{21} \cdot \vec{x}_{20}}{x_{21}^2 \, x_{20}^2} \left[\mathbf{1} - U_{\vec{x}_{1\perp}} U^\dagger_{\vec{x}_{2\perp}} - U_{\vec{x}_{2\perp}} U^\dagger_{\vec{x}_{0\perp}} + U_{\vec{x}_{1\perp}} U^\dagger_{\vec{x}_{0\perp}} \right]^{ab}$$

$$\nu^a_{\vec{x}_{1\perp}} = \frac{i}{g \, \pi^2} \int \frac{d^2x_2}{x_{21}^2} \, \mathrm{Tr} \left[T^a U_{\vec{x}_{1\perp}} U^\dagger_{\vec{x}_{2\perp}} \right]$$

- Here U is the adjoint Wilson line on a light cone,

$$U_{\vec{x}_\perp} = \mathrm{P} \exp \left\{ i \, g \int\limits_{-\infty}^{\infty} dx^- \, \mathcal{A}^+(x^+ = 0, x^-, \vec{x}_\perp) \right\}$$

The JIMWLK Equation

- JIMWLK equation can be used to construct any-N_C small-x evolution of any operator made of infinite light-cone Wilson lines (in any representation), such as color-dipole, color-quadrupole, etc., and other operators.

- Since

$$\Box\alpha(x^-, \vec{x}) = \rho(x^-, \vec{x})$$

  JIMWLK evolution can be re-written in terms of the color density ρ in the kernel.

- JIMWLK approach sums up powers of $\alpha_s Y$ and $\alpha_s^2 A^{1/3}$

Solution of BK equation

Unitarity: $N \leq 1$

We conclude that

$$Q_s^2 \sim \left(\frac{1}{x}\right)^{\lambda}$$

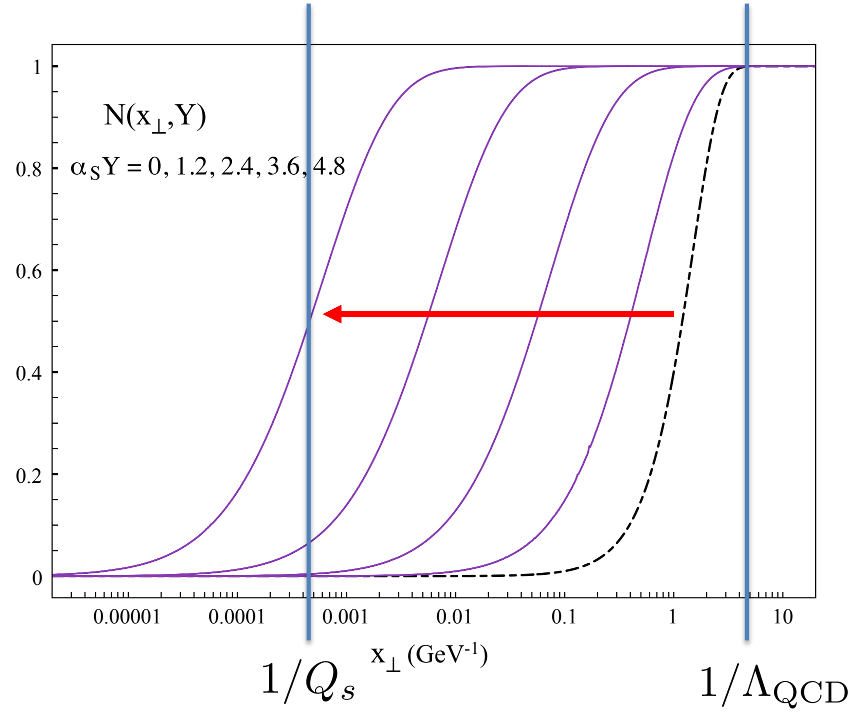

numerical solution
by J. Albacete '03

Energy increases → Q_s increases
moving further away from Λ_{QCD}

BK solution preserves the black disk limit, N<1 always
(unlike the linear BFKL equation)

$$\sigma^{q\bar{q}A} = 2 \int d^2b \, N(x_\perp, b_\perp, Y)$$

Sub-Eikonal Operators

Dipole picture of DIS

$$W^{\mu\nu} = \frac{1}{4\pi M_p} \int d^4x \, e^{iq\cdot x} \, \langle P | j^\mu(x) \, j^\nu(0) | P \rangle$$

$$q^\mu = \left(\frac{Q^2}{2q^-}, q^-, 0_\perp \right)$$

Large q^- → large x^- separation

$$e^{iq\cdot x} = e^{i\frac{Q^2}{2q^-}x^- + iq^- x^+}$$

$$x^\pm = \frac{t \pm z}{\sqrt{2}}$$

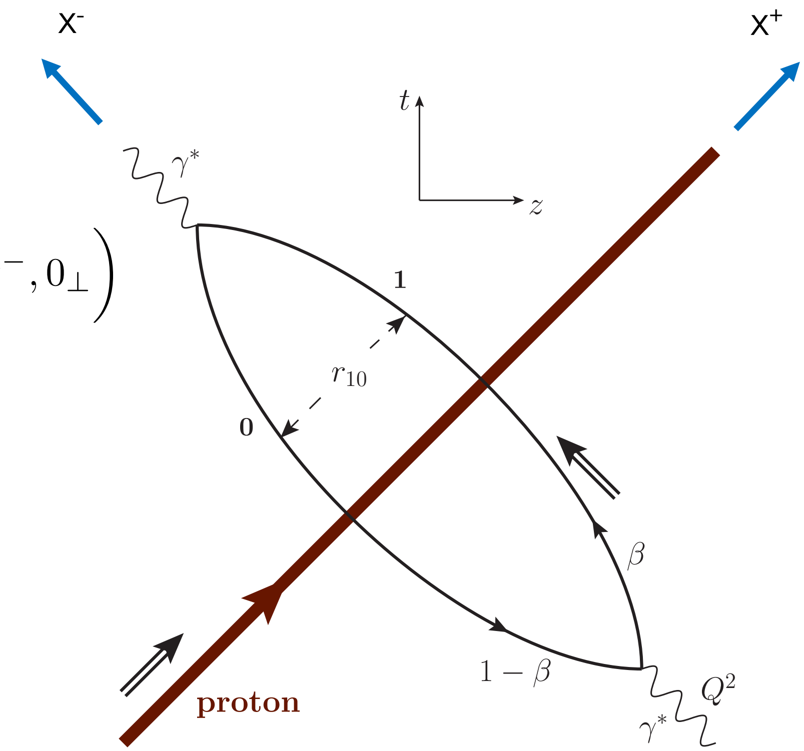

aka the "shock wave"

Polarized Dipole: non-eikonal small-x physics

- All flavor-singlet small-x helicity observables depend on "polarized dipole amplitudes":

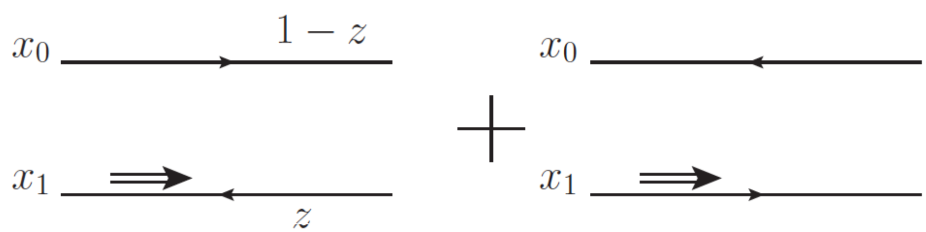

$$G_{10}(z) \equiv \frac{1}{2N_c} \operatorname{Re} \left\langle\!\!\left\langle \mathrm{T}\,\mathrm{tr}\left[V_{\underline{0}} V_{\underline{1}}^{pol\,\dagger}\right] + \mathrm{T}\,\mathrm{tr}\left[V_{\underline{1}}^{pol} V_{\underline{0}}^{\dagger}\right] \right\rangle\!\!\right\rangle(z)$$

unpolarized quark

polarized quark: eikonal propagation, non-eikonal spin-dependent interaction

$$V_{\underline{x}} = \mathcal{P} \exp\left[ig \int\limits_{-\infty}^{\infty} dx^- A^+(0^+, x^-, \underline{x}) \right]$$

- Double brackets denote an object with energy suppression scaled out:

$$\left\langle\!\!\left\langle \mathcal{O} \right\rangle\!\!\right\rangle(z) \equiv zs \left\langle \mathcal{O} \right\rangle(z)$$

Polarized fundamental "Wilson line"

- To complete the definition of the polarized dipole amplitude, we need to construct the definition of the polarized "Wilson line" V^{pol}, which is the leading helicity-dependent contribution for the quark scattering amplitude on a longitudinally-polarized target proton.

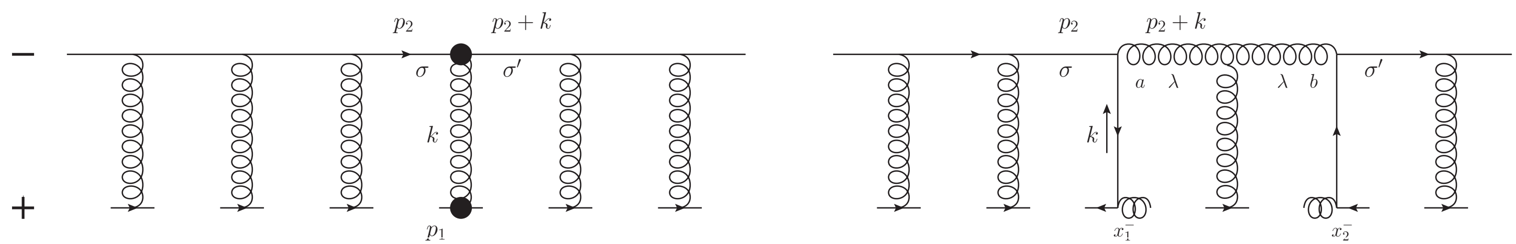

- At the leading order we can either exchange one non-eikonal *t*-channel gluon (with quark-gluon vertices denoted by blobs above) to transfer polarization between the projectile and the target, or two *t*-channel quarks, as shown above.
- We employ a blend of Brodsky & Lepage's LCPT and background field method-inspired operator treatment. We refer to the latter as the **light-cone operator treatment (LCOT)**.

Notation

- Fundamental light-cone Wilson line:

$$V_{\underline{x}}[b^-, a^-] = \text{P}\exp\left\{ig \int\limits_{a^-}^{b^-} dx^- \, A^+(x^-, \underline{x})\right\}$$

- Adjoint light-cone Wilson line:

$$U_{\underline{x}}[b^-, a^-] = \mathcal{P}\exp\left[ig \int\limits_{a^-}^{b^-} dx^- \, \mathcal{A}^+(x^+ = 0, x^-, \underline{x})\right]$$

- They sum multiple eikonal re-scatterings to all orders.

Eikonality

- One can classify various quantities (e.g.,TMDs) by their small-*x* asymptotics.
- Eikonal behavior corresponds to (up to ~α_S corrections in the power) $f(x, k_T^2) \sim \frac{1}{x}$
  Examples: unpolarized TMDs, Sivers function.
- Sub-eikonal behavior corresponds to $g(x, k_T^2) \sim \left(\frac{1}{x}\right)^0 = \text{const}$
  Example: helicity TMDs.
- Sub-sub-eikonal behavior is $h(x, k_T^2) \sim x$
  Examples: transversity, Boer-Mulder function.
- We've been calling the leading power of x "eikonality".

Sub-eikonal quark S-matrix in background gluon and quark fields

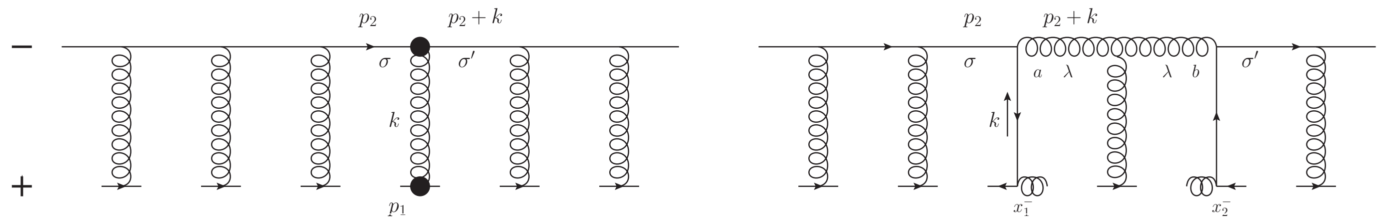

- The full sub-eikonal S-matrix for massless quarks is (Balitsky&Tarasov '15; KPS '17; YK, Sievert, '18; Chirilli '18; Altinoluk et al, '20; YK, Santiago '21)

$$V_{\underline{x},\underline{y};\sigma',\sigma} = V_{\underline{x}}\, \delta^2(\underline{x}-\underline{y})\, \delta_{\sigma,\sigma'}$$

"helicity independent" "helicity dependent"

$$-\vec{\mu}\cdot\vec{B} = -\mu_z\, B_z = \mu_z\, F^{12}$$

$$+\frac{i\,P^+}{s}\int\limits_{-\infty}^{\infty} dz^- d^2z\; V_{\underline{x}}[\infty, z^-]\, \delta^2(\underline{x}-\underline{z})\, \left[-\delta_{\sigma,\sigma'}\, \overleftarrow{D}^i\, D^i + g\,\sigma\,\delta_{\sigma,\sigma'}\, F^{12}\right](z^-,\underline{z})\, V_{\underline{y}}[z^-,-\infty]\, \delta^2(\underline{y}-\underline{z})$$

$$-\frac{g^2 P^+}{2s}\delta^2(\underline{x}-\underline{y})\int\limits_{-\infty}^{\infty} dz_1^- \int\limits_{z_1^-}^{\infty} dz_2^-\, V_{\underline{x}}[\infty, z_2^-]\, t^b \psi_\beta(z_2^-,\underline{x})\, U_{\underline{x}}^{ba}[z_2^-, z_1^-]\left[\delta_{\sigma,\sigma'}\gamma^+ - \sigma\delta_{\sigma,\sigma'}\gamma^+\gamma^5\right]_{\alpha\beta}\bar{\psi}_\alpha(z_1^-,\underline{x})\, t^a V_{\underline{x}}[z_1^-,-\infty]$$

"helicity independent" "helicity dependent"

Longitudinal momentum transfer

In addition to the above, there is x+ dependence in the regular Wilson line, which is usually neglected in the eikonal approximation. If we expand in x+, we get a sub-eikonal correction

$$\int_{-\infty}^{\infty} dx^+ \, e^{-i(p_f^- - p_i^-)\, x^+} \, V_{\underline{x}}(x^+) = \int_{-\infty}^{\infty} dx^+ \, e^{-i(p_f^- - p_i^-)\, x^+} \, \left[V_{\underline{x}}(0^+) + x^+ \, \partial^- V_{\underline{x}}(0^+) + \ldots \right]$$

$$= 2\pi \, \delta(p_f^- - p_i^-) \, V_{\underline{x}}(0^+) - 2\pi \, i \left[\frac{\partial}{\partial p_f^-} \delta(p_f^- - p_i^-) \right] 2 \sqrt{p_f^- \, p_i^-} \, V_{\underline{x}}^{\mathrm{G}[3]} + \ldots .$$

where we have introduced another “helicity-independent: sub-eikonal operator (Altinoluk et al, ’20)

$$V_{\underline{x}}^{\mathrm{G}[3]} = \frac{i \, g \, P^+}{s} \int_{-\infty}^{\infty} dx^- V_{\underline{x}}[\infty, x^-] \, F^{+-}(x^-, \underline{x}) \; V_{\underline{x}}[x^-, -\infty].$$

This operator does not contribute to small-x helicity evolution at the leading order (DLA).

Helicity Distributions and Observables at Small x

Dipole Gluon Helicity TMD

- We start with the definition of the gluon dipole helicity TMD, corresponding to the Jaffe-Manohar PDF ΔG,

$$g_1^G(x, k_T^2) = \frac{-2i\, S_L}{x\, P^+} \int \frac{d\xi^- \, d^2\xi}{(2\pi)^3} \, e^{ixP^+ \xi^- - i\underline{k}\cdot\underline{\xi}} \left\langle P, S_L | \epsilon_T^{ij} \, \mathrm{tr} \left[F^{+i}(0) \, \mathcal{U}^{[+]\dagger}[0,\xi] \, F^{+j}(\xi) \, \mathcal{U}^{[-]}[\xi, 0] \right] | P, S_L \right\rangle_{\xi^+=0}$$

- Here $U^{[+]}$ and $U^{[-]}$ are future and past-pointing Wilson line staples (hence the name 'dipole' TMD, F. Dominguez et al '11 – looks like a dipole scattering on a proton):

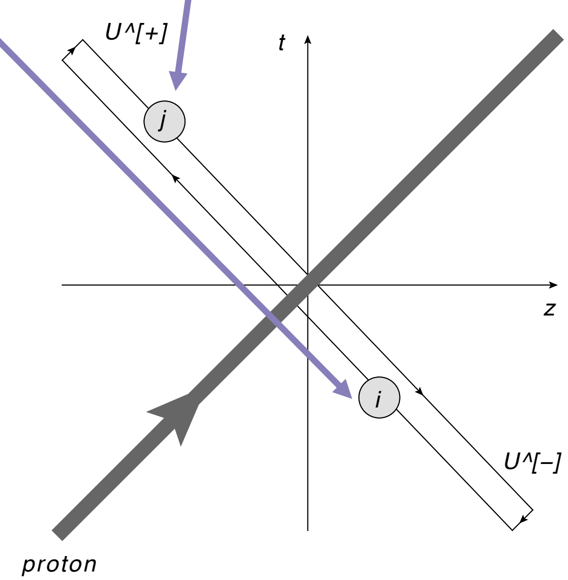

Gluon Helicity

- A calculation gives

$$\Delta G(x, Q^2) = \frac{2N_c}{\alpha_s \pi^2} \, G_2 \left(\frac{1}{Q^2}, zs = \frac{Q^2}{x} \right)$$

$$g_{1L}^{G\,dip}(x, k_T^2) = \frac{N_c}{\alpha_s 2\pi^4} \int d^2 x_{10} \, e^{-i\underline{k}\cdot\underline{x}_{10}} \, G_2 \left(x_{10}^2, zs = \frac{Q^2}{x} \right)$$

- Here we defined a new dipole amplitude G_2 (cf. Hatta et al, 2016; KPS 2017)

$$\int d^2 \left(\frac{x_1 + x_0}{2} \right) \, G_{10}^i(zs) = (x_{10})_\perp^i \, G_1(x_{10}^2, zs) + \epsilon^{ij} \, (x_{10})_\perp^j \, G_2(x_{10}^2, zs)$$

$$G_{10}^j(zs) \equiv \frac{1}{2N_c} \left\langle\!\!\left\langle \mathrm{tr} \left[V_{\underline{0}}^\dagger \, V_{\underline{1}}^{j\,\mathrm{G}[2]} + \left(V_{\underline{1}}^{j\,\mathrm{G}[2]} \right)^\dagger V_{\underline{0}} \right] \right\rangle\!\!\right\rangle$$

$$V_{\underline{z}}^{i\,\mathrm{G}[2]} \equiv \frac{P^+}{2s} \int\limits_{-\infty}^{\infty} dz^- \, V_{\underline{z}}[\infty, z^-] \left[D^i(z^-, \underline{z}) - \overleftarrow{D}^i (z^-, \underline{z}) \right] V_{\underline{z}}[z^-, -\infty]$$

What is this D-D operator? Turns out it is related to the DD operator from before.

Quark Helicity PDF and TMD

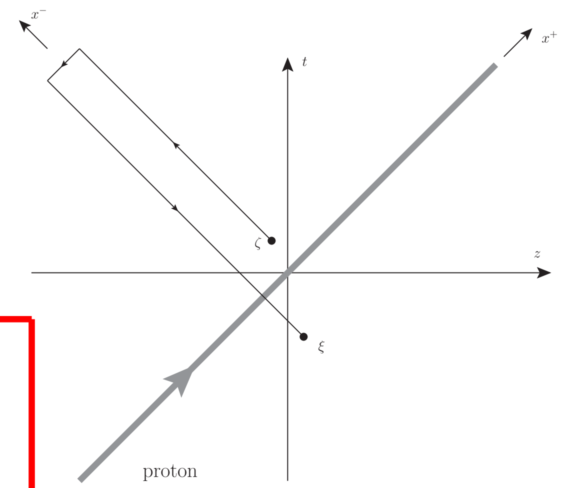

- The flavor-singlet quark helicity PDF and TMD are

$$\Delta\Sigma(x, Q^2) = \frac{N_f}{\alpha_s \, \pi^2} \, \widetilde{Q}\left(x_{10}^2 = \frac{1}{Q^2}, s = \frac{Q^2}{x} \right)$$

$$g_{1L}^S(x, k_T^2) = \frac{1}{4\pi^4 \alpha_s} \int d^2 x_{10} \, e^{-i \underline{k} \cdot \underline{x}_{10}} \; \widetilde{Q}(x_{10}^2, Q^2/x)$$

- We have defined another operator:

$$\widetilde{Q}_{12}(s) \equiv \left\langle \left\langle \frac{g^2}{16\sqrt{k^- p_2^-}} \int\limits_{-\infty}^{\infty} dy^- \int\limits_{-\infty}^{\infty} dz^- \left[\bar{\psi}(y^-, \underline{x}_2) \left(\frac{1}{2} \gamma^+ \gamma^5 \right) V_{\underline{2}}[y^-, \infty] \, V_{\underline{1}}[\infty, z^-] \, \psi(z^-, \underline{x}_1) \right. \right. \right.$$
$$\left. \left. \left. + \bar{\psi}(y^-, \underline{x}_2) \left(\frac{1}{2} \gamma^+ \gamma^5 \right) V_{\underline{2}}[y^-, -\infty] \, V_{\underline{1}}[-\infty, z^-] \, \psi(z^-, \underline{x}_1) + \text{c.c.} \right] \right\rangle \right\rangle (s).$$

g_1 structure function

- g_1 structure function is obtained similarly, using DIS in the dipole picture:

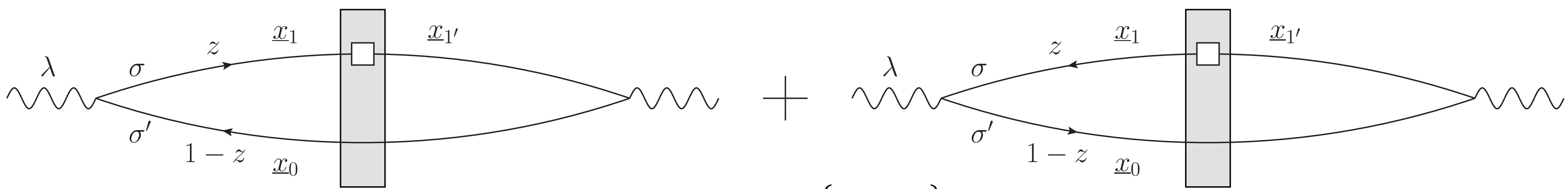

- One gets $$g_1(x,Q^2) = -\sum_f \frac{N_c\, Z_f^2}{4\pi^3} \int\limits_{\Lambda^2/s}^{1} \frac{dz}{z} \int\limits_{\frac{1}{zs}}^{\min\left\{\frac{1}{zQ^2}, \frac{1}{\Lambda^2}\right\}} \frac{dx_{10}^2}{x_{10}^2} \left[Q(x_{10}^2, zs) + 2\, G_2(x_{10}^2, zs)\right]$$
- G_2 was defined before. This is the gluon admixture to quark helicity distributions.
- The dipole amplitude Q is due to F^{12} & axial current.
- The contribution of G_2 comes from the DD operator in the quark S-matrix.
- Hence, the DD operator is related to the Jaffe-Manohar distribution.

Amplitude Q

$$Q(x_{10}^2, zs) \equiv \int d^2 \left(\frac{x_0 + x_1}{2} \right) Q_{10}(zs)$$

- The amplitude Q is defined by

$$Q_{10}(zs) \equiv \frac{1}{2N_c} \, \text{Re} \left\langle\!\!\left\langle \text{T tr} \left[V_{\underline{0}} \, V_{\underline{1}}^{\text{pol}[1] \, \dagger} \right] + \text{T tr} \left[V_{\underline{1}}^{\text{pol}[1]} \, V_{\underline{0}}^{\dagger} \right] \right\rangle\!\!\right\rangle$$

with $V_{\underline{x}}^{\text{pol}[1]} = V_{\underline{x}}^{\text{G}[1]} + V_{\underline{x}}^{\text{q}[1]}$, where

$$V_{\underline{x}}^{\text{G}[1]} = \frac{i \, g \, P^+}{s} \int\limits_{-\infty}^{\infty} dx^- V_{\underline{x}}[\infty, x^-] \, F^{12}(x^-, \underline{x}) \; V_{\underline{x}}[x^-, -\infty]$$

$$V_{\underline{x}}^{\text{q}[1]} = \frac{g^2 P^+}{2 \, s} \int\limits_{-\infty}^{\infty} dx_1^- \int\limits_{x_1^-}^{\infty} dx_2^- \, V_{\underline{x}}[\infty, x_2^-] \, t^b \, \psi_\beta(x_2^-, \underline{x}) \, U_{\underline{x}}^{ba}[x_2^-, x_1^-] \; \left[\gamma^+ \gamma^5\right]_{\alpha\beta} \; \bar{\psi}_\alpha(x_1^-, \underline{x}) \, t^a \, V_{\underline{x}}[x_1^-, -\infty]$$

- U = adjoint light-cone Wilson line.

Helicity Evolution

Evolution for Polarized Quark Dipole

One can construct an evolution equation for the polarized dipole:

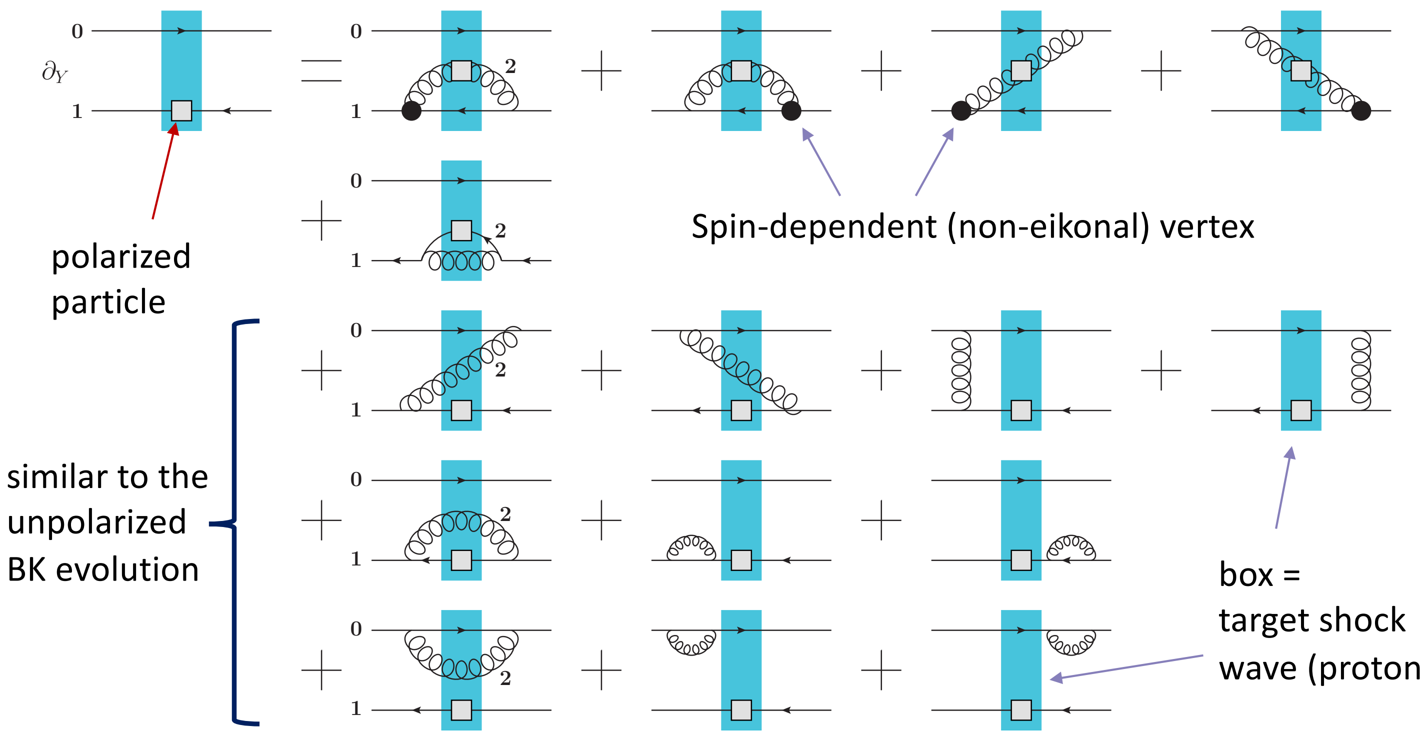

Large N_c

- At large-N_c the equations close (Q → G).
- Everything with 2 in the subscript (e.g., G_2 and Γ_2) is new (CTT+K) compared to the KPS ('15-'18) papers.

$$G(x_{10}^2, zs) = G^{(0)}(x_{10}^2, zs) + \frac{\alpha_s N_c}{2\pi} \int\limits_{\frac{1}{s x_{10}^2}}^{z} \frac{dz'}{z'} \int\limits_{\frac{1}{z's}}^{x_{10}^2} \frac{dx_{21}^2}{x_{21}^2} \Big[\Gamma(x_{10}^2, x_{21}^2, z's) + 3\, G(x_{21}^2, z's) + 2\, G_2(x_{21}^2, z's) + 2\, \Gamma_2(x_{10}^2, x_{21}^2, z's) \Big],$$

$$\Gamma(x_{10}^2, x_{21}^2, z's) = G^{(0)}(x_{10}^2, z's) + \frac{\alpha_s N_c}{2\pi} \int\limits_{\frac{1}{s x_{10}^2}}^{z'} \frac{dz''}{z''} \int\limits_{\frac{1}{z''s}}^{\min\left[x_{10}^2, x_{21}^2 \frac{z'}{z''}\right]} \frac{dx_{32}^2}{x_{32}^2} \Big[\Gamma(x_{10}^2, x_{32}^2, z''s) + 3\, G(x_{32}^2, z''s) + 2\, G_2(x_{32}^2, z''s) + 2\, \Gamma_2(x_{10}^2, x_{32}^2, z''s) \Big],$$

$$G_2(x_{10}^2, zs) = G_2^{(0)}(x_{10}^2, zs) + \frac{\alpha_s N_c}{\pi} \int\limits_{\frac{\Lambda^2}{s}}^{z} \frac{dz'}{z'} \int\limits_{\max\left[x_{10}^2, \frac{1}{z's}\right]}^{\min\left[\frac{z}{z'} x_{10}^2, \frac{1}{\Lambda^2}\right]} \frac{dx_{21}^2}{x_{21}^2} \left[G(x_{21}^2, z's) + 2\, G_2(x_{21}^2, z's) \right],$$

$$\Gamma_2(x_{10}^2, x_{21}^2, z's) = G_2^{(0)}(x_{10}^2, z's) + \frac{\alpha_s N_c}{\pi} \int\limits_{\frac{\Lambda^2}{s}}^{z' \frac{x_{21}^2}{x_{10}^2}} \frac{dz''}{z''} \int\limits_{\max\left[x_{10}^2, \frac{1}{z''s}\right]}^{\min\left[\frac{z'}{z''} x_{21}^2, \frac{1}{\Lambda^2}\right]} \frac{dx_{32}^2}{x_{32}^2} \left[G(x_{32}^2, z''s) + 2\, G_2(x_{32}^2, z''s) \right]$$

Initial Conditions

- The initial conditions are given by the Born-level graphs

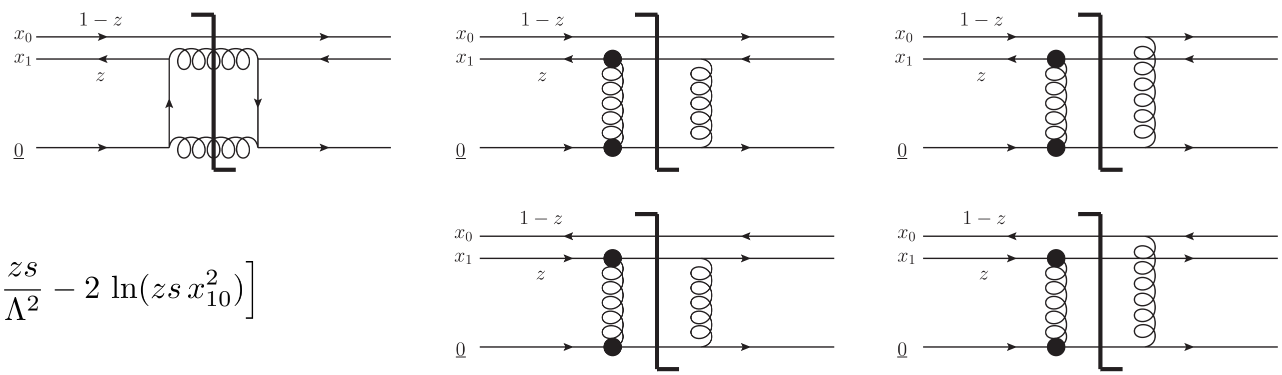

$$G^{(0)}(x_{10}^2, z) = \frac{\alpha_s^2 C_F}{N_c} \pi \left[C_F \ln \frac{zs}{\Lambda^2} - 2 \ln(zs\, x_{10}^2) \right]$$

$$\Gamma^{(0)}(x_{10}^2, x_{21}^2, z) = G^{(0)}(x_{10}^2, z)$$

- Similar Born-level calculation is done for G_2 and Γ_2.

"Neighbor" dipole

- There is a new object in the evolution equation – **the neighbor dipole amplitude**.
- This is specific for the DLA evolution. Gluon emission may happen in one dipole, but, due to lifetime ordering, may 'know' about another dipole:

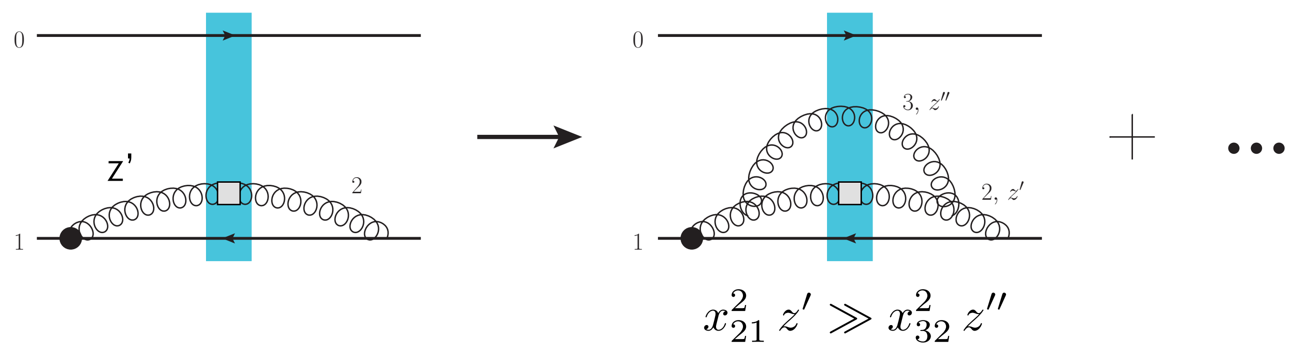

- We denote the evolution in the neighbor dipole 02 by $\Gamma_{02,\,21}(z')$

Helicity Evolution Ingredients

- Unlike the unpolarized evolution, in one step of helicity evolution we may emit a soft gluon or a soft quark (all in $A^-=0$ LC gauge of the projectile):

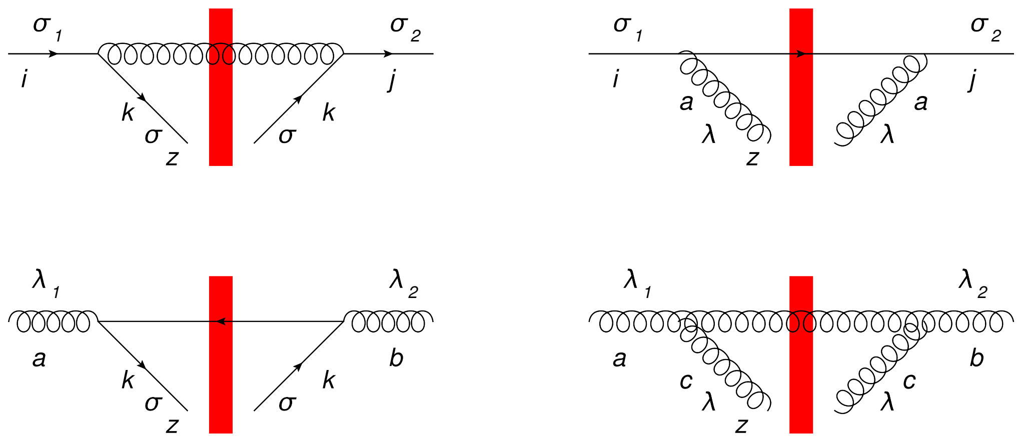

- When emitting gluons, one emission is eikonal, while another one is soft, but non-eikonal, as is needed to transfer polarization down the cascade/ladder.

Helicity Evolution: Ladders

- To get an idea of how the helicity evolution works let us try iterating the splitting kernels by considering ladder diagrams (circles denote non-eikonal gluon vertices):

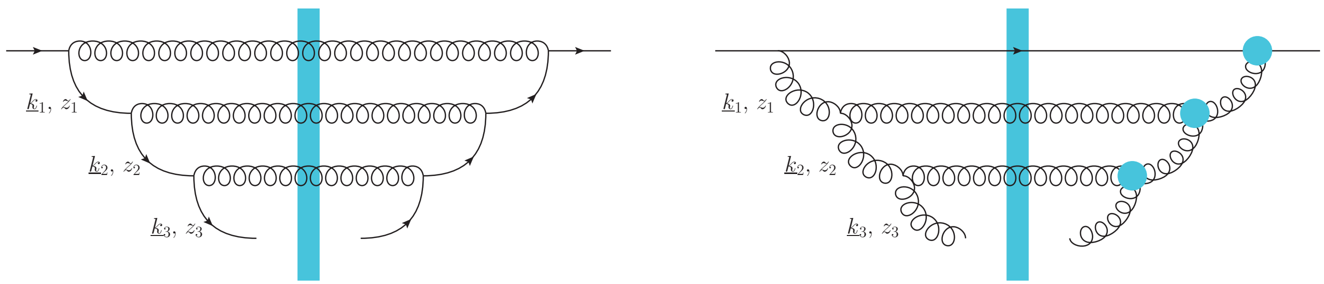

- To get the leading-energy asymptotics we need to order the longitudinal momentum fractions of the quarks and gluons (just like in the unpolarized evolution case) $1 \gg z_1 \gg z_2 \gg z_3 \gg \ldots$

  obtaining a nested integral $$\alpha_s^3 \int\limits_{z_i}^{1} \frac{dz_1}{z_1} \int\limits_{z_i}^{z_1} \frac{dz_2}{z_2} \int\limits_{z_i}^{z_2} \frac{dz_3}{z_3}\, z_3 \otimes \frac{1}{z_3\, s} \sim \frac{1}{s}\, \alpha_s^3\, \ln^3 s$$

Helicity Evolution: Ladders

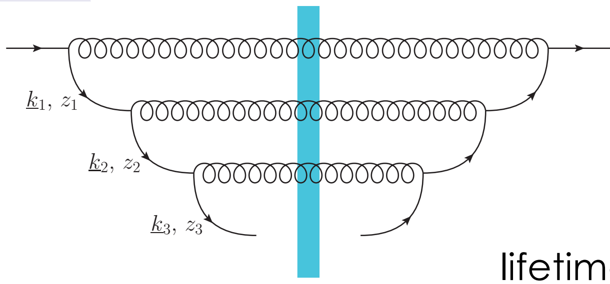

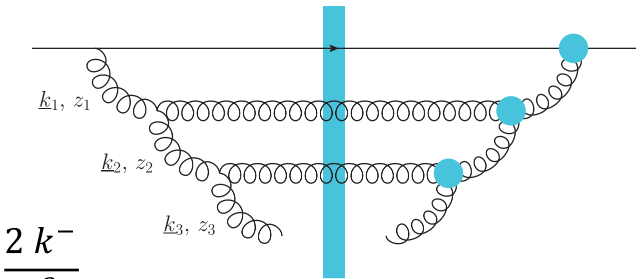

lifetime = $\dfrac{2\, k^-}{k_\perp^2}$

- However, these are not all the logs of energy one can get here. Transverse momentum (or distance) integrals have UV and IR divergences, which lead to logs of energy as well.
- If we order gluon/quark lifetimes as (Sudakov-β ordering) $\frac{2k_1^-}{\underline{k}_1^2} \gg \frac{2k_2^-}{\underline{k}_2^2} \gg \frac{2k_3^-}{\underline{k}_3^2} \gg \ldots$ then ($z_i = k_i^-/p^-$). $\frac{\underline{k}_1^2}{z_1} \ll \frac{\underline{k}_2^2}{z_2} \ll \frac{\underline{k}_3^2}{z_3} \ll \ldots$ and $z_1\, \underline{x}_1^2 \gg z_2\, \underline{x}_2^2 \gg z_3\, \underline{x}_3^2 \gg \ldots$

  we would get integrals like $\displaystyle\int\limits_{1/(z_n\, s)}^{x_{n-1,\perp}^2\, z_{n-1}/z_n} \frac{dx_{n,\perp}^2}{x_{n,\perp}^2}$ also generating logs of energy.

Helicity Evolution: Ladders

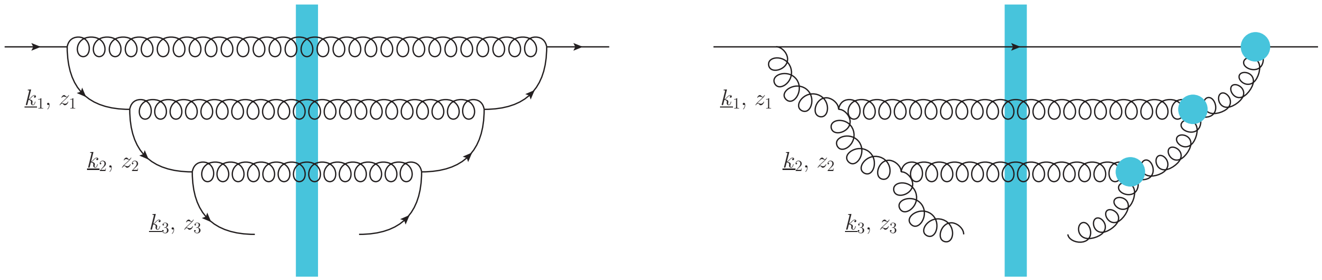

- To summarize, the above ladder diagrams are parametrically of the order

$$\frac{1}{s}\,\alpha_s^3\,\ln^6 s$$

- Note two features:
    - 1/s suppression due to non-eikonal exchange
    - two logs of energy per each power of the coupling!

Resummation Parameter

- For helicity evolution the leading resummation parameter is different from BFKL, BK or JIMWLK, which resum powers of leading logarithms (LLA)

$$\alpha_s \ \ln(1/x)$$

- Helicity evolution resummation parameter is double-logarithmic (DLA):

$$\alpha_s \ \ln^2 \frac{1}{x}$$

- The second logarithm of x arises due to transverse momentum (or transverse coordinate) integration being logarithmic both in the UV and IR.

- This was known before: Kirschner and Lipatov '83; Kirschner '84; Bartels, Ermolaev, Ryskin '95, '96; Griffiths and Ross '99; Itakura et al '03; Bartels and Lublinsky '03.

Large-N_c&N_f Evolution

- Helicity evolution equations also close in the large-N_c&N_f (Veneziano) limit.
- To derive those, need to add the transition diagrams (J. Borden, YK, M. Li, ‘24):

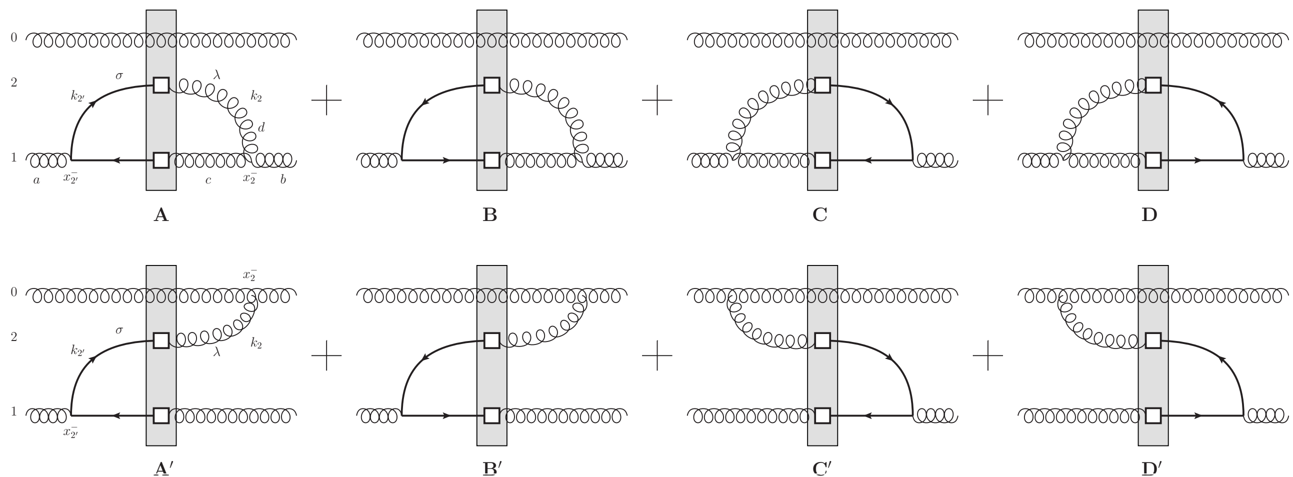

Large-N_c&N_f

- Large-N_c&N_f limit is more realistic as it includes quarks.
- Everything with 2 in the subscript (e.g., G_2 and Γ_2) is new (CTT-K) compared to the KPS ('15-'18) papers.
- Blue is the contribution of transition operators (BCL).
- These equations agree with polarized DGLAP anomalous dimensions at small x to all three known loops.

$$\begin{aligned} Q(x_{10}^2, zs) = Q^{(0)}(x_{10}^2, zs) &+ \frac{\alpha_s N_c}{2\pi} \int_{1/sx_{10}^2}^{z} \frac{dz'}{z'} \int_{1/z's}^{x_{10}^2} \frac{dx_{21}^2}{x_{21}^2} \Big[2\,\widetilde{G}(x_{21}^2, z's) + 2\,\widetilde{\Gamma}(x_{10}^2, x_{21}^2, z's) \\ &+ Q(x_{21}^2, z's) - \overline{\Gamma}(x_{10}^2, x_{21}^2, z's) + 2\,\Gamma_2(x_{10}^2, x_{21}^2, z's) + 2\,G_2(x_{21}^2, z's) \Big] \\ &+ \frac{\alpha_s N_c}{4\pi} \int_{\Lambda^2/s}^{z} \frac{dz'}{z'} \int_{1/z's}^{\min\{x_{10}^2 z/z', 1/\Lambda^2\}} \frac{dx_{21}^2}{x_{21}^2} \left[Q(x_{21}^2, z's) + 2\,G_2(x_{21}^2, z's) \right], \end{aligned} \tag{76a}$$

$$\begin{aligned} \overline{\Gamma}(x_{10}^2, x_{21}^2, z's) = Q^{(0)}(x_{10}^2, z's) &+ \frac{\alpha_s N_c}{2\pi} \int_{1/sx_{10}^2}^{z'} \frac{dz''}{z''} \int_{1/z''s}^{\min\{x_{10}^2, x_{21}^2 z'/z''\}} \frac{dx_{32}^2}{x_{32}^2} \Big[2\,\widetilde{G}(x_{32}^2, z''s) \\ &+ 2\,\widetilde{\Gamma}(x_{10}^2, x_{32}^2, z''s) + Q(x_{32}^2, z''s) - \overline{\Gamma}(x_{10}^2, x_{32}^2, z''s) + 2\,\Gamma_2(x_{10}^2, x_{32}^2, z''s) + 2\,G_2(x_{32}^2, z''s) \Big] \\ &+ \frac{\alpha_s N_c}{4\pi} \int_{\Lambda^2/s}^{z'} \frac{dz''}{z''} \int_{1/z''s}^{\min\{x_{21}^2 z'/z'', 1/\Lambda^2\}} \frac{dx_{32}^2}{x_{32}^2} \left[Q(x_{32}^2, z''s) + 2\,G_2(x_{32}^2, z''s) \right], \end{aligned} \tag{76b}$$

$$\begin{aligned} \widetilde{G}(x_{10}^2, zs) = \widetilde{G}^{(0)}(x_{10}^2, zs) &+ \frac{\alpha_s N_c}{2\pi} \int_{1/sx_{10}^2}^{z} \frac{dz'}{z'} \int_{1/z's}^{x_{10}^2} \frac{dx_{21}^2}{x_{21}^2} \Big[3\,\widetilde{G}(x_{21}^2, z's) + \widetilde{\Gamma}(x_{10}^2, x_{21}^2, z's) \\ &+ 2\,G_2(x_{21}^2, z's) + \left(2 - \frac{N_f}{2N_c}\right) \Gamma_2(x_{10}^2, x_{21}^2, z's) - \frac{N_f}{4N_c} \overline{\Gamma}(x_{10}^2, x_{21}^2, z's) - \frac{N_f}{2N_c} \widetilde{Q}(x_{21}^2, z's) \Big] \\ &- \frac{\alpha_s N_f}{8\pi} \int_{\Lambda^2/s}^{z} \frac{dz'}{z'} \int_{\max\{x_{10}^2, 1/z's\}}^{\min\{x_{10}^2 z/z', 1/\Lambda^2\}} \frac{dx_{21}^2}{x_{21}^2} \left[Q(x_{21}^2, z's) + 2\,G_2(x_{21}^2, z's) \right], \end{aligned} \tag{76c}$$

$$\begin{aligned} \widetilde{\Gamma}(x_{10}^2, x_{21}^2, z's) = \widetilde{G}^{(0)}(x_{10}^2, z's) &+ \frac{\alpha_s N_c}{2\pi} \int_{1/sx_{10}^2}^{z'} \frac{dz''}{z''} \int_{1/z''s}^{\min\{x_{10}^2, x_{21}^2 z'/z''\}} \frac{dx_{32}^2}{x_{32}^2} \Big[3\,\widetilde{G}(x_{32}^2, z''s) \\ + \widetilde{\Gamma}(x_{10}^2, x_{32}^2, z''s) + 2\,G_2(x_{32}^2, z''s) &+ \left(2 - \frac{N_f}{2N_c}\right) \Gamma_2(x_{10}^2, x_{32}^2, z''s) - \frac{N_f}{4N_c} \overline{\Gamma}(x_{10}^2, x_{32}^2, z''s) - \frac{N_f}{2N_c} \widetilde{Q}(x_{32}^2, z''s) \Big] \\ &- \frac{\alpha_s N_f}{8\pi} \int_{\Lambda^2/s}^{z' x_{21}^2/x_{10}^2} \frac{dz''}{z''} \int_{\max\{x_{10}^2, 1/z''s\}}^{\min\{x_{21}^2 z'/z'', 1/\Lambda^2\}} \frac{dx_{32}^2}{x_{32}^2} \left[Q(x_{32}^2, z''s) + 2\,G_2(x_{32}^2, z''s) \right], \end{aligned} \tag{76d}$$

$$G_2(x_{10}^2, zs) = G_2^{(0)}(x_{10}^2, zs) + \frac{\alpha_s N_c}{\pi} \int_{\frac{\Lambda^2}{s}}^{z} \frac{dz'}{z'} \int_{\max\left[x_{10}^2, \frac{1}{z's}\right]}^{\min\{\frac{z}{z'} x_{10}^2, 1/\Lambda^2\}} \frac{dx_{21}^2}{x_{21}^2} \left[\widetilde{G}(x_{21}^2, z's) + 2\,G_2(x_{21}^2, z's) \right], \tag{76e}$$

$$\Gamma_2(x_{10}^2, x_{21}^2, z's) = G_2^{(0)}(x_{10}^2, z's) + \frac{\alpha_s N_c}{\pi} \int_{\frac{\Lambda^2}{s}}^{z' \frac{x_{21}^2}{x_{10}^2}} \frac{dz''}{z''} \int_{\max\left[x_{10}^2, \frac{1}{z''s}\right]}^{\min\{\frac{z'}{z''} x_{21}^2, 1/\Lambda^2\}} \frac{dx_{32}^2}{x_{32}^2} \left[\widetilde{G}(x_{32}^2, z''s) + 2\,G_2(x_{32}^2, z''s) \right], \tag{76f}$$

$$\widetilde{Q}(x_{10}^2, zs) = \widetilde{Q}^{(0)}(x_{10}^2, zs) - \frac{\alpha_s N_c}{2\pi} \int_{\frac{\Lambda^2}{s}}^{z} \frac{dz'}{z'} \int_{\max\left[x_{10}^2, \frac{1}{z's}\right]}^{\min\{\frac{z}{z'} x_{10}^2, 1/\Lambda^2\}} \frac{dx_{21}^2}{x_{21}^2} \left[Q(x_{21}^2, z's) + 2\,G_2(x_{21}^2, z's) \right]. \tag{76g}$$

Small-x Asymptotics

Solution of the Large-N_c Equations

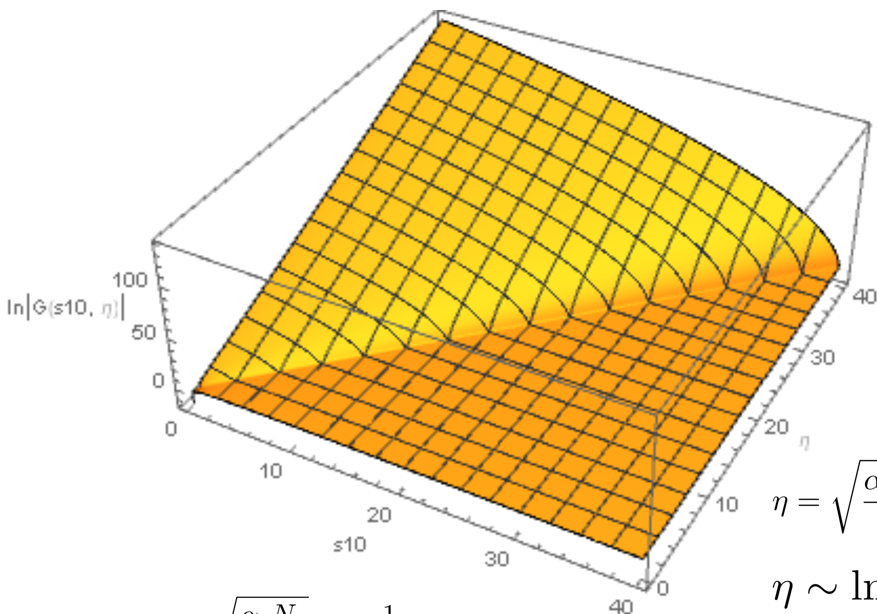

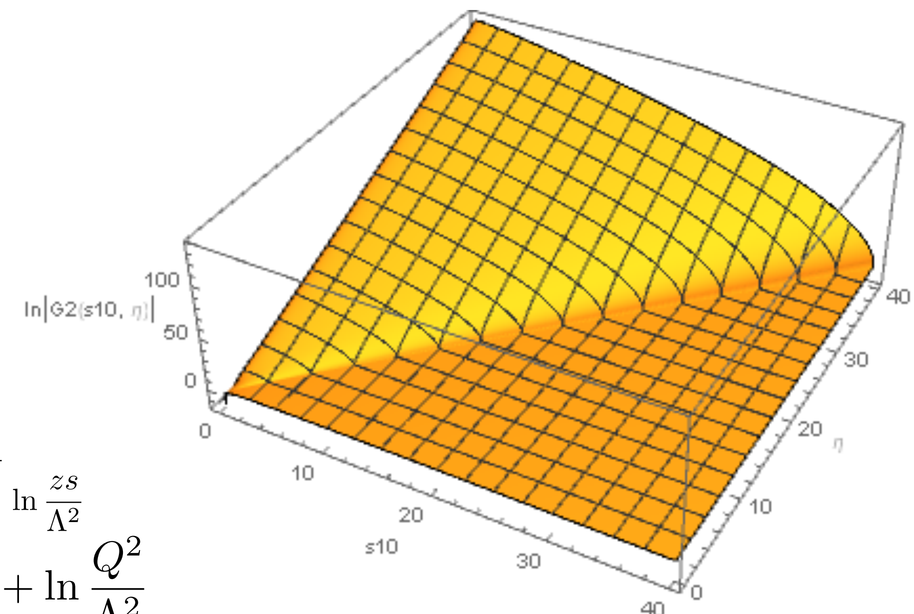

$$s_{10} = \sqrt{\frac{\alpha_s N_c}{2\pi}} \ln \frac{1}{x_{10}^2 \Lambda^2}$$

$$s_{10} \sim \ln \frac{Q^2}{\Lambda^2}$$

$$\eta = \sqrt{\frac{\alpha_s N_c}{2\pi}} \ln \frac{zs}{\Lambda^2}$$

$$\eta \sim \ln \frac{1}{x} + \ln \frac{Q^2}{\Lambda^2}$$

The large-N_c equations for G and G_2 can be solved numerically (and, possibly, analytically).

Small-x Asymptotics

- Fitting the slope of the log plots of G and G_2 vs e we can read off the small-x intercept (the power of x):

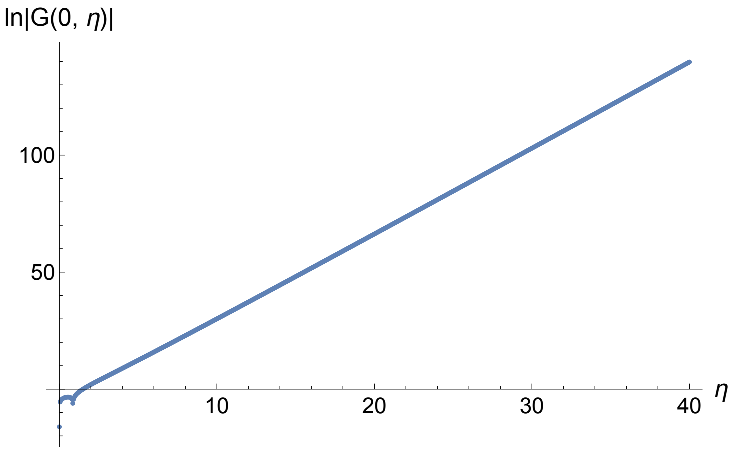

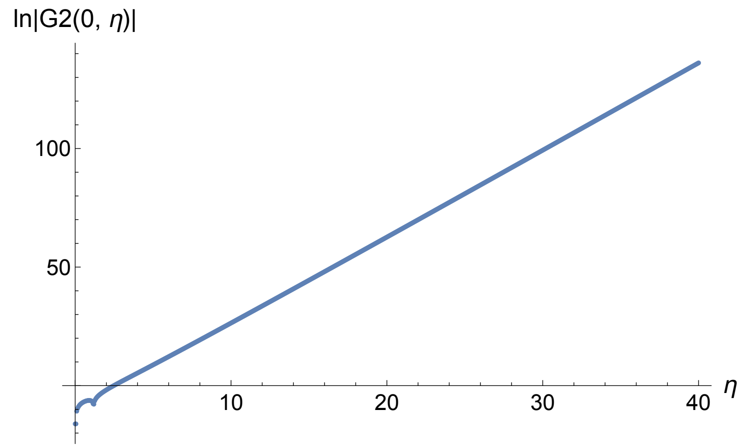

F. Cougoulic, YK, A. Tarasov, Y. Tawabutr, 2022

Small-x Asymptotics for Helicity Distributions

- The resulting small-x asymptotics for helicity PDFs and the g_1 structure function at large N_c is

$$\Delta\Sigma(x, Q^2) \sim \Delta G(x, Q^2) \sim g_1(x, Q^2) \sim \left(\frac{1}{x}\right)^{3.66\,\sqrt{\frac{\alpha_s\,N_c}{2\pi}}}$$

- This power (aka the intercept) is in complete agreement with the work by J. Bartels, B. Ermolaev, and M. Ryskin (BER, 1996) using infrared evolution equations (with the analytic intercept constructed by KPS in 2016):

$$\alpha_h = \sqrt{\frac{17+\sqrt{97}}{2}}\,\sqrt{\frac{\alpha_s\,N_c}{2\pi}} \approx 3.664\,\sqrt{\frac{\alpha_s\,N_c}{2\pi}}$$

- "Peace in the valley."
- **Right?**

Analytic Solution of the Large-N_c Equations

- We want to solve these equations:

$$G(x_{10}^2, zs) = G^{(0)}(x_{10}^2, zs) + \frac{\alpha_s N_c}{2\pi} \int\limits_{\frac{1}{s x_{10}^2}}^{z} \frac{dz'}{z'} \int\limits_{\frac{1}{z' s}}^{x_{10}^2} \frac{dx_{21}^2}{x_{21}^2} \Big[\Gamma(x_{10}^2, x_{21}^2, z's) + 3\, G(x_{21}^2, z's) + 2\, G_2(x_{21}^2, z's) + 2\, \Gamma_2(x_{10}^2, x_{21}^2, z's) \Big],$$

$$\Gamma(x_{10}^2, x_{21}^2, z's) = G^{(0)}(x_{10}^2, z's) + \frac{\alpha_s N_c}{2\pi} \int\limits_{\frac{1}{s x_{10}^2}}^{z'} \frac{dz''}{z''} \int\limits_{\frac{1}{z'' s}}^{\min\left[x_{10}^2, x_{21}^2 \frac{z'}{z''}\right]} \frac{dx_{32}^2}{x_{32}^2} \Big[\Gamma(x_{10}^2, x_{32}^2, z''s) + 3\, G(x_{32}^2, z''s) + 2\, G_2(x_{32}^2, z''s) + 2\, \Gamma_2(x_{10}^2, x_{32}^2, z''s) \Big],$$

$$G_2(x_{10}^2, zs) = G_2^{(0)}(x_{10}^2, zs) + \frac{\alpha_s N_c}{\pi} \int\limits_{\frac{\Lambda^2}{s}}^{z} \frac{dz'}{z'} \int\limits_{\max\left[x_{10}^2, \frac{1}{z's}\right]}^{\min\left[\frac{z}{z'} x_{10}^2, \frac{1}{\Lambda^2}\right]} \frac{dx_{21}^2}{x_{21}^2} \left[G(x_{21}^2, z's) + 2\, G_2(x_{21}^2, z's) \right],$$

$$\Gamma_2(x_{10}^2, x_{21}^2, z's) = G_2^{(0)}(x_{10}^2, z's) + \frac{\alpha_s N_c}{\pi} \int\limits_{\frac{\Lambda^2}{s}}^{z' \frac{x_{21}^2}{x_{10}^2}} \frac{dz''}{z''} \int\limits_{\max\left[x_{10}^2, \frac{1}{z''s}\right]}^{\min\left[\frac{z'}{z''} x_{21}^2, \frac{1}{\Lambda^2}\right]} \frac{dx_{32}^2}{x_{32}^2} \left[G(x_{32}^2, z''s) + 2\, G_2(x_{32}^2, z''s) \right]$$

Analytic Solution of the Large-N$_c$ Equations

- The strategy is to use the double Laplace transform,

$$\bar{\alpha}_s \equiv \frac{\alpha_s N_c}{2\pi}$$

$$G_2(x_{10}^2, zs) = \int \frac{d\omega}{2\pi i} \int \frac{d\gamma}{2\pi i} \, e^{\omega \ln(zsx_{10}^2) + \gamma \ln\left(\frac{1}{x_{10}^2 \Lambda^2}\right)} \, G_{2\omega\gamma}$$

- One gets the expressions for all the other dipole amplitudes this way, for instance

$$G(x_{10}^2, zs) = \int \frac{d\omega}{2\pi i} \int \frac{d\gamma}{2\pi i} \, e^{\omega \ln(zsx_{10}^2) + \gamma \ln\left(\frac{1}{x_{10}^2 \Lambda^2}\right)} \left[\frac{\omega\gamma}{2\,\bar{\alpha}_s} \left(G_{2\omega\gamma} - G_{2\omega\gamma}^{(0)} \right) - 2\, G_{2\omega\gamma} \right]$$

- Neighbor amplitudes involve several different double Laplace transforms:

$$\Gamma_2(x_{10}^2, x_{21}^2, z's) = \int \frac{d\omega}{2\pi i} \int \frac{d\gamma}{2\pi i} \left[e^{\omega \ln(z'sx_{21}^2) + \gamma \ln\left(\frac{1}{x_{10}^2 \Lambda^2}\right)} \left(G_{2\omega\gamma} - G_{2\omega\gamma}^{(0)} \right) + e^{\omega \ln(z'sx_{10}^2) + \gamma \ln\left(\frac{1}{x_{10}^2 \Lambda^2}\right)} \, G_{2\omega\gamma}^{(0)} \right]$$

Analytic Solution of the Large-N_c Equations

- In the end, all the amplitudes in the double-Laplace space can be expressed in terms of the initial conditions/inhomogeneous terms, e.g.,

$$G_{2\omega\gamma} = G^{(0)}_{2\omega\gamma} + \frac{\bar{\alpha}_s}{\omega\left(\gamma - \gamma^-_\omega\right)\left(\gamma - \gamma^+_\omega\right)} \Bigg[2\left(\gamma - \delta^+_\omega\right)\left(G^{(0)}_{\delta^+_\omega \gamma} + 2\, G^{(0)}_{2\,\delta^+_\omega \gamma}\right) - 2\left(\gamma^+_\omega - \delta^+_\omega\right)\left(G^{(0)}_{\delta^+_\omega \gamma^+_\omega} + 2\, G^{(0)}_{2\,\delta^+_\omega \gamma^+_\omega}\right) + 8\,\delta^-_\omega \left(G^{(0)}_{2\omega\gamma} - G^{(0)}_{2\omega\gamma^+_\omega}\right)\Bigg]$$

with

$$\delta^\pm_\omega = \frac{\omega}{2}\left[1 \pm \sqrt{1 - \frac{4\,\bar{\alpha}_s}{\omega^2}}\right] \qquad \gamma^\pm_\omega = \frac{\omega}{2}\left[1 \pm \sqrt{1 - \frac{16\,\bar{\alpha}_s}{\omega^2}\sqrt{1 - \frac{4\,\bar{\alpha}_s}{\omega^2}}}\right]$$

- More details in J. Borden, YK, 2304.06161 [hep-ph].

Small-x Asymptotics for Helicity Distributions

- Let's take a closer look at the anomalous dimension:

$$\Delta G(x, Q^2) = \int \frac{d\omega}{2\pi i} \left(\frac{1}{x} \right)^{\omega} \left(\frac{Q^2}{\Lambda^2} \right)^{\Delta \gamma_{GG}(\omega)} \Delta G_{\omega}(\Lambda^2)$$

- In the pure-glue case, Bartels, Ermolaev and Ryskin's (BER) anomalous dimension can be found analytically. It reads (KPS '16)

$$\Delta \gamma_{GG}^{BER}(\omega) = \frac{1}{2} \left[\omega - \sqrt{\omega^2 - 16\, \bar{\alpha}_s \frac{1 - \frac{3\, \bar{\alpha}_s}{\omega^2}}{1 - \frac{\bar{\alpha}_s}{\omega^2}}} \right] \qquad \bar{\alpha}_s = \frac{\alpha_s\, N_c}{2\pi}$$

- Our evolution's anomalous dimension can be found analytically at large-N_c (J. Borden, YK, 2304.06161 [hep-ph]):

$$\Delta \gamma_{GG}^{us}(\omega) = \frac{1}{2} \left[\omega - \sqrt{\omega^2 - 16\, \bar{\alpha}_s \sqrt{1 - \frac{4\, \bar{\alpha}_s}{\omega^2}}} \right]$$

A Tale of Two Anomalous Dimensions

- The two anomalous dimensions look similar enough but are not the same function.

$$\Delta\gamma_{GG}^{BER}(\omega) = \frac{1}{2}\left[\omega - \sqrt{\omega^2 - 16\,\bar{\alpha}_s \frac{1 - \frac{3\,\bar{\alpha}_s}{\omega^2}}{1 - \frac{\bar{\alpha}_s}{\omega^2}}}\right] \qquad \Delta\gamma_{GG}^{us}(\omega) = \frac{1}{2}\left[\omega - \sqrt{\omega^2 - 16\,\bar{\alpha}_s\sqrt{1 - \frac{4\,\bar{\alpha}_s}{\omega^2}}}\right]$$

- Their expansions in α_s start out the same, then differ at four (!) loops (the first 3 terms agree with the existing finite-order calculations, the four-loop result is unknown):

$$\Delta\gamma_{GG}^{BER}(\omega) = \underline{\frac{4\,\bar{\alpha}_s}{\omega} + \frac{8\,\bar{\alpha}_s^2}{\omega^3} + \frac{56\,\bar{\alpha}_s^3}{\omega^5}} + \underline{\frac{504\,\bar{\alpha}_s^4}{\omega^7}} + \ldots$$

$$\Delta\gamma_{GG}^{us}(\omega) = \underline{\frac{4\,\bar{\alpha}_s}{\omega} + \frac{8\,\bar{\alpha}_s^2}{\omega^3} + \frac{56\,\bar{\alpha}_s^3}{\omega^5}} + \underline{\frac{496\,\bar{\alpha}_s^4}{\omega^7}} + \ldots$$

A Tale of Two Intercepts

$$\Delta G(x,Q^2) = \int \frac{d\omega}{2\pi i} \left(\frac{1}{x}\right)^{\omega} \left(\frac{Q^2}{\Lambda^2}\right)^{\Delta\gamma_{GG}(\omega)} \Delta G_{\omega}(\Lambda^2)$$

$$\Delta\gamma_{GG}^{BER}(\omega) = \frac{1}{2}\left[\omega - \sqrt{\omega^2 - 16\,\bar{\alpha}_s \frac{1-\frac{3\,\bar{\alpha}_s}{\omega^2}}{1-\frac{\bar{\alpha}_s}{\omega^2}}}\right] \qquad \Delta\gamma_{GG}^{us}(\omega) = \frac{1}{2}\left[\omega - \sqrt{\omega^2 - 16\,\bar{\alpha}_s\sqrt{1-\frac{4\,\bar{\alpha}_s}{\omega^2}}}\right]$$

- The intercept (largest power Re[ω]) is given by the right-most singularity (branch point) of the anomalous dimension.
- For BER this gives $\alpha_h = \sqrt{\frac{17+\sqrt{97}}{2}}\sqrt{\frac{\alpha_s N_c}{2\pi}} \approx 3.664\sqrt{\frac{\alpha_s N_c}{2\pi}}$
- For us $\alpha_h = \frac{4}{3^{1/3}}\sqrt{\mathrm{Re}\left[(-9+i\sqrt{111})^{1/3}\right]}\sqrt{\frac{\alpha_s N_c}{2\pi}} \approx 3.661\sqrt{\frac{\alpha_s N_c}{2\pi}}$

A Tale of Two Intercepts

$$\Delta\Sigma(x, Q^2)\Big|_{x\ll 1} \sim \Delta G(x, Q^2)\Big|_{x\ll 1} \sim \left(\frac{1}{x}\right)^{\alpha_h}$$

- The power α_h is known as the intercept.
- BER:

$$\alpha_h = \sqrt{\frac{17+\sqrt{97}}{2}}\sqrt{\frac{\alpha_s N_c}{2\pi}} \approx 3.664\sqrt{\frac{\alpha_s N_c}{2\pi}}$$

- Us:

$$\alpha_h = \frac{4}{3^{1/3}}\sqrt{\mathrm{Re}\left[(-9+i\sqrt{111})^{1/3}\right]}\sqrt{\frac{\alpha_s N_c}{2\pi}} \approx 3.661\sqrt{\frac{\alpha_s N_c}{2\pi}}$$

- Our numerical solution also gave the intercept of 3.660 or 3.661, but we believed we had larger error bars.
- We (still) disagree with BER. Albeit in the 3rd decimal point…

Phenomenology

D. Adamiak, N. Baldonado, YK, W. Melnitchouk, D. Pitonyak, N. Sato, M. Sievert, A. Tarasov, Y. Tawabutr, = JAMsmallx, 2308.07461 [hep-ph], 2503.21006 [hep-ph]

Polarized DIS and SIDIS data

- We can use the large-N_c&N_f version of the evolution to fit all the existing world polarized DIS and SIDIS data.
- Why not large-N_c? Have to distinguish a true quark dipole from the subset of the gluon one. Need to extract all helicity PDFs for light quark flavors, in addition to the gluon helicity PDF.
- Hence, the quark amplitudes Q_q come with the flavor index q.
- Drawback: many dipole amplitudes, hard to constrain all.
- LO intercept is large: had to include running coupling (not shown) into the evolution.

$$Q(x_{10}^2, zs) = Q^{(0)}(x_{10}^2, zs) + \frac{\alpha_s N_c}{2\pi} \int_{1/sx_{10}^2}^{z} \frac{dz'}{z'} \int_{1/z's}^{x_{10}^2} \frac{dx_{21}^2}{x_{21}^2} \Big[2\,\widetilde{G}(x_{21}^2, z's) + 2\,\widetilde{\Gamma}(x_{10}^2, x_{21}^2, z's) + Q(x_{21}^2, z's) - \overline{\Gamma}(x_{10}^2, x_{21}^2, z's) + 2\,\Gamma_2(x_{10}^2, x_{21}^2, z's) + 2\,G_2(x_{21}^2, z's) \Big] + \frac{\alpha_s N_c}{4\pi} \int_{\Lambda^2/s}^{z} \frac{dz'}{z'} \int_{1/z's}^{\min\{x_{10}^2 z/z', 1/\Lambda^2\}} \frac{dx_{21}^2}{x_{21}^2} \left[Q(x_{21}^2, z's) + 2\,G_2(x_{21}^2, z's) \right], \tag{76a}$$

$$\overline{\Gamma}(x_{10}^2, x_{21}^2, z's) = Q^{(0)}(x_{10}^2, z's) + \frac{\alpha_s N_c}{2\pi} \int_{1/sx_{10}^2}^{z'} \frac{dz''}{z''} \int_{1/z''s}^{\min\{x_{10}^2, x_{21}^2 z'/z''\}} \frac{dx_{32}^2}{x_{32}^2} \Big[2\,\widetilde{G}(x_{32}^2, z''s) + 2\,\widetilde{\Gamma}(x_{10}^2, x_{32}^2, z''s) + Q(x_{32}^2, z''s) - \overline{\Gamma}(x_{10}^2, x_{32}^2, z''s) + 2\,\Gamma_2(x_{10}^2, x_{32}^2, z''s) + 2\,G_2(x_{32}^2, z''s) \Big] + \frac{\alpha_s N_c}{4\pi} \int_{\Lambda^2/s}^{z'} \frac{dz''}{z''} \int_{1/z''s}^{\min\{x_{21}^2 z'/z'', 1/\Lambda^2\}} \frac{dx_{32}^2}{x_{32}^2} \left[Q(x_{32}^2, z''s) + 2\,G_2(x_{32}^2, z''s) \right], \tag{76b}$$

$$\widetilde{G}(x_{10}^2, zs) = \widetilde{G}^{(0)}(x_{10}^2, zs) + \frac{\alpha_s N_c}{2\pi} \int_{1/sx_{10}^2}^{z} \frac{dz'}{z'} \int_{1/z's}^{x_{10}^2} \frac{dx_{21}^2}{x_{21}^2} \Big[3\,\widetilde{G}(x_{21}^2, z's) + \widetilde{\Gamma}(x_{10}^2, x_{21}^2, z's) + 2\,G_2(x_{21}^2, z's) + \left(2 - \frac{N_f}{2N_c}\right) \Gamma_2(x_{10}^2, x_{21}^2, z's) - \frac{N_f}{4N_c}\,\overline{\Gamma}(x_{10}^2, x_{21}^2, z's) - \frac{N_f}{2N_c}\,\widetilde{Q}(x_{21}^2, z's) \Big] - \frac{\alpha_s N_f}{8\pi} \int_{\Lambda^2/s}^{z} \frac{dz'}{z'} \int_{\max\{x_{10}^2, 1/z's\}}^{\min\{x_{10}^2 z/z', 1/\Lambda^2\}} \frac{dx_{21}^2}{x_{21}^2} \left[Q(x_{21}^2, z's) + 2\,G_2(x_{21}^2, z's) \right], \tag{76c}$$

$$\widetilde{\Gamma}(x_{10}^2, x_{21}^2, z's) = \widetilde{G}^{(0)}(x_{10}^2, z's) + \frac{\alpha_s N_c}{2\pi} \int_{1/sx_{10}^2}^{z'} \frac{dz''}{z''} \int_{1/z''s}^{\min\{x_{10}^2, x_{21}^2 z'/z''\}} \frac{dx_{32}^2}{x_{32}^2} \Big[3\,\widetilde{G}(x_{32}^2, z''s) + \widetilde{\Gamma}(x_{10}^2, x_{32}^2, z''s) + 2\,G_2(x_{32}^2, z''s) + \left(2 - \frac{N_f}{2N_c}\right) \Gamma_2(x_{10}^2, x_{32}^2, z''s) - \frac{N_f}{4N_c}\,\overline{\Gamma}(x_{10}^2, x_{32}^2, z''s) - \frac{N_f}{2N_c}\,\widetilde{Q}(x_{32}^2, z''s) \Big] - \frac{\alpha_s N_f}{8\pi} \int_{\Lambda^2/s}^{z' x_{21}^2/x_{10}^2} \frac{dz''}{z''} \int_{\max\{x_{10}^2, 1/z''s\}}^{\min\{x_{21}^2 z'/z'', 1/\Lambda^2\}} \frac{dx_{32}^2}{x_{32}^2} \left[Q(x_{32}^2, z''s) + 2\,G_2(x_{32}^2, z''s) \right], \tag{76d}$$

$$G_2(x_{10}^2, zs) = G_2^{(0)}(x_{10}^2, zs) + \frac{\alpha_s N_c}{\pi} \int\limits_{\frac{\Lambda^2}{s}}^{z} \frac{dz'}{z'} \int\limits_{\max\left[x_{10}^2, \frac{1}{z's}\right]}^{\min\{\frac{z}{z'} x_{10}^2, 1/\Lambda^2\}} \frac{dx_{21}^2}{x_{21}^2} \left[\widetilde{G}(x_{21}^2, z's) + 2\,G_2(x_{21}^2, z's) \right], \tag{76e}$$

$$\Gamma_2(x_{10}^2, x_{21}^2, z's) = G_2^{(0)}(x_{10}^2, z's) + \frac{\alpha_s N_c}{\pi} \int\limits_{\frac{\Lambda^2}{s}}^{z' \frac{x_{21}^2}{x_{10}^2}} \frac{dz''}{z''} \int\limits_{\max\left[x_{10}^2, \frac{1}{z''s}\right]}^{\min\{\frac{z'}{z''} x_{21}^2, 1/\Lambda^2\}} \frac{dx_{32}^2}{x_{32}^2} \left[\widetilde{G}(x_{32}^2, z''s) + 2\,G_2(x_{32}^2, z''s) \right], \tag{76f}$$

$$\widetilde{Q}(x_{10}^2, zs) = \widetilde{Q}^{(0)}(x_{10}^2, zs) - \frac{\alpha_s N_c}{2\pi} \int\limits_{\frac{\Lambda^2}{s}}^{z} \frac{dz'}{z'} \int\limits_{\max\left[x_{10}^2, \frac{1}{z's}\right]}^{\min\{\frac{z}{z'} x_{10}^2, 1/\Lambda^2\}} \frac{dx_{21}^2}{x_{21}^2} \left[Q(x_{21}^2, z's) + 2\,G_2(x_{21}^2, z's) \right]. \tag{76g}$$

Polarized SIDIS at small x

Consider (anti-)quark production in the current fragmentation region in the polarized e+p scattering at small x.

The process is similar to the g_1 structure function calculation.

A straightforward calculation yields the SIDIS structure function (D_1 = fragmentation function)

$$g_1^h(x,z,Q^2) \approx \frac{1}{2}\sum_{q,\bar{q}} e_q^2\, \Delta q(x,Q^2)\, D_1^{h/q}(z,Q^2)$$

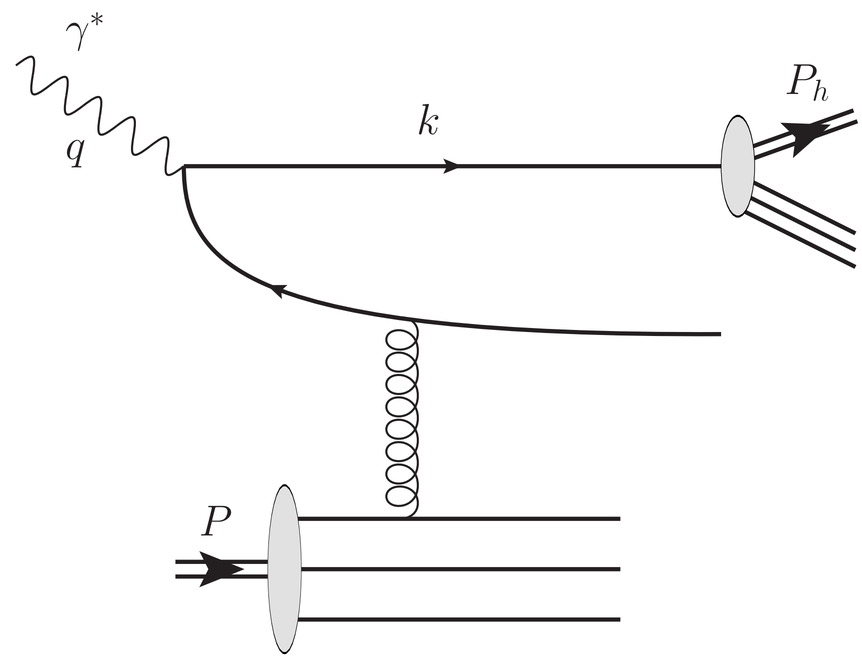

JAMsmallx: **Adamiak**, Baldonado, YK, Melnitchouk, Pitonyak, Sato, Sievert, Tarasov, Tawabutr, 2308.07461 [hep-ph]

$5 \times 10^{-3} < x < 0.1 \equiv x_0$

The analysis

$\chi^2/N_{pts} = 1.03$

$1.69 \text{ GeV}^2 < Q^2 < 10.4 \text{ GeV}^2$

Initial conditions: $Q^{(0)}(x_{10}^2, zs) \sim G_2^{(0)}(x_{10}^2, zs) \sim a \ln \frac{zs}{\Lambda^2} + b \ln \frac{1}{x_{10}^2 \Lambda^2} + c$

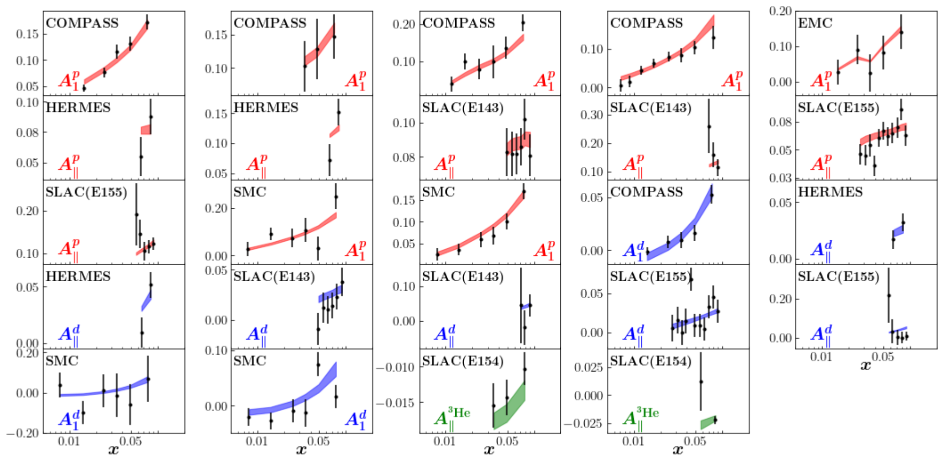

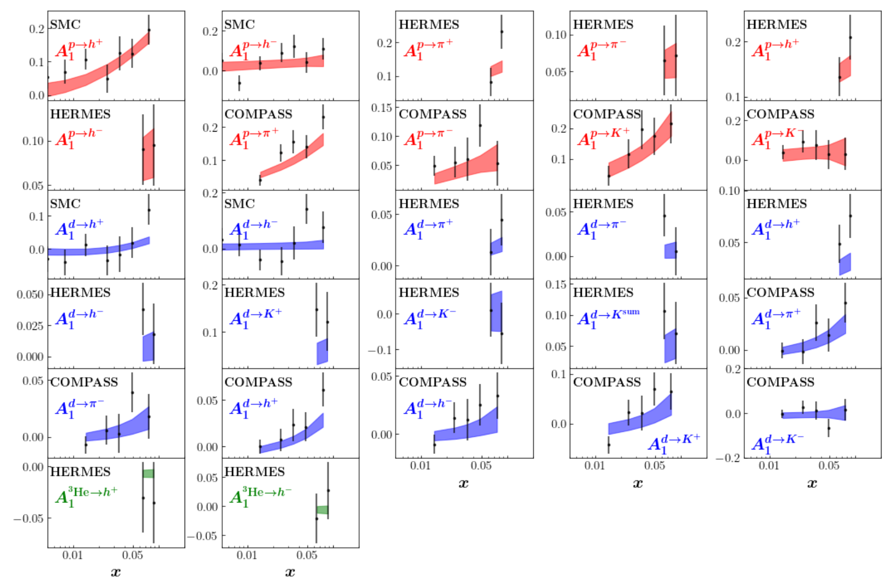

$$A_{\|} = \frac{\sigma^{\downarrow\Uparrow} - \sigma^{\uparrow\Uparrow}}{\sigma^{\downarrow\Uparrow} + \sigma^{\uparrow\Uparrow}} \qquad A_1 \approx \frac{g_1}{F_1}$$

$$A_{\|} \approx D\, A_1$$

Double-spin asymmetries for p, d, and ^{3}He

D= kinematic factor (known)
Running-coupling large-N_c&N_f evolution, 226 polarized DIS and SIDIS data points.

Proton g_1 structure function

JAM-smallx

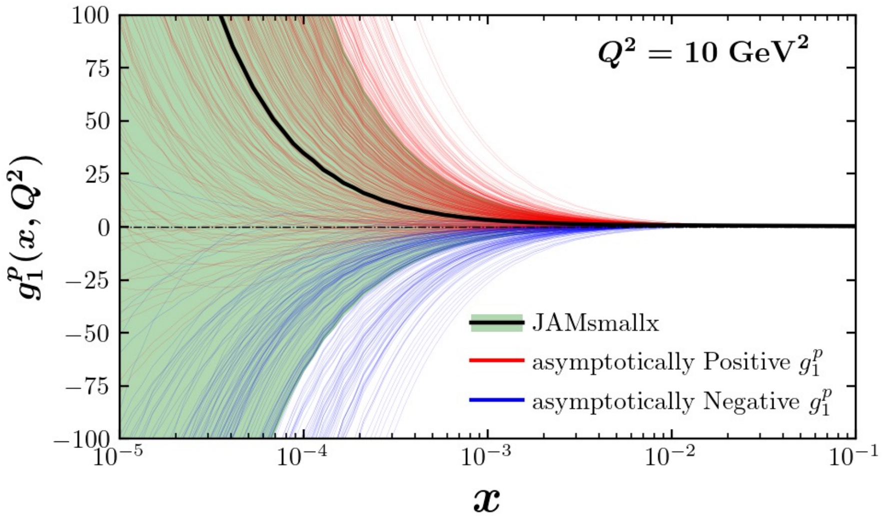

g_1^p extracted from the existing data

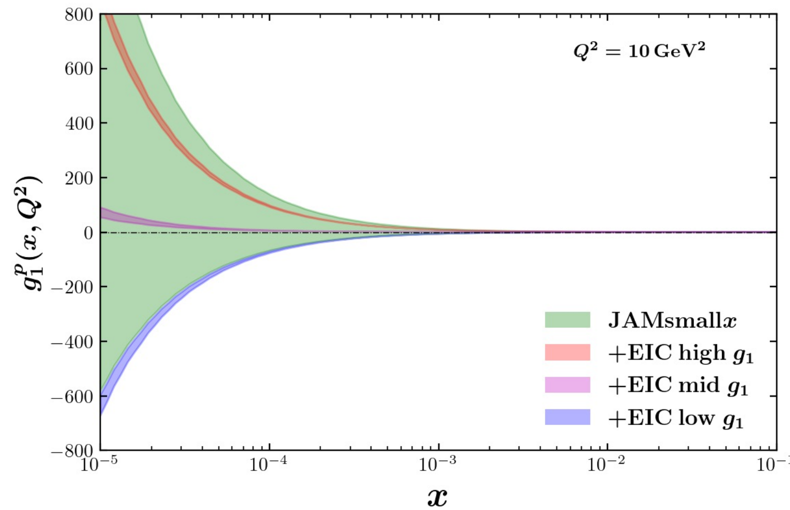

EIC impact

- JAM is based on a Bayesian Monte-Carlo: it uses replicas.
- Due to the lack of constraints, the spread is large.
- On the right, extraction using EIC pseudo-data (3 thin bands = 3 possible EIC data sets).

Helicity PDFs:

JAM-smallx

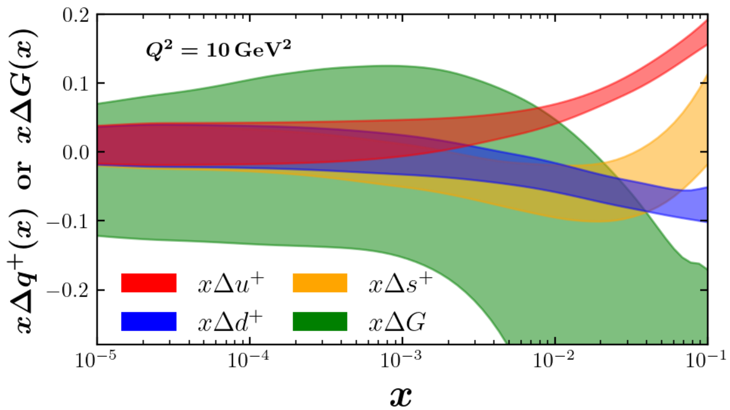

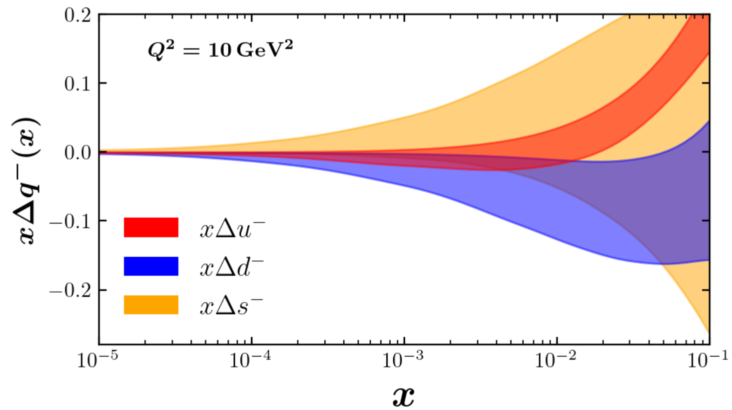

$$\Delta q^+ = \Delta q + \Delta\bar{q} \qquad \Delta q^- = \Delta q - \Delta\bar{q}$$

Uncertainties at small x seem to be driven by our inability to constrain the dipole amplitude G_2 and Gtilde using the current data.

JAMsmallx: Adamiak, Baldonado, YK, Melnitchouk, Pitonyak, Sato, Sievert, Tarasov, Tawabutr 2023

How much spin is there at small x?

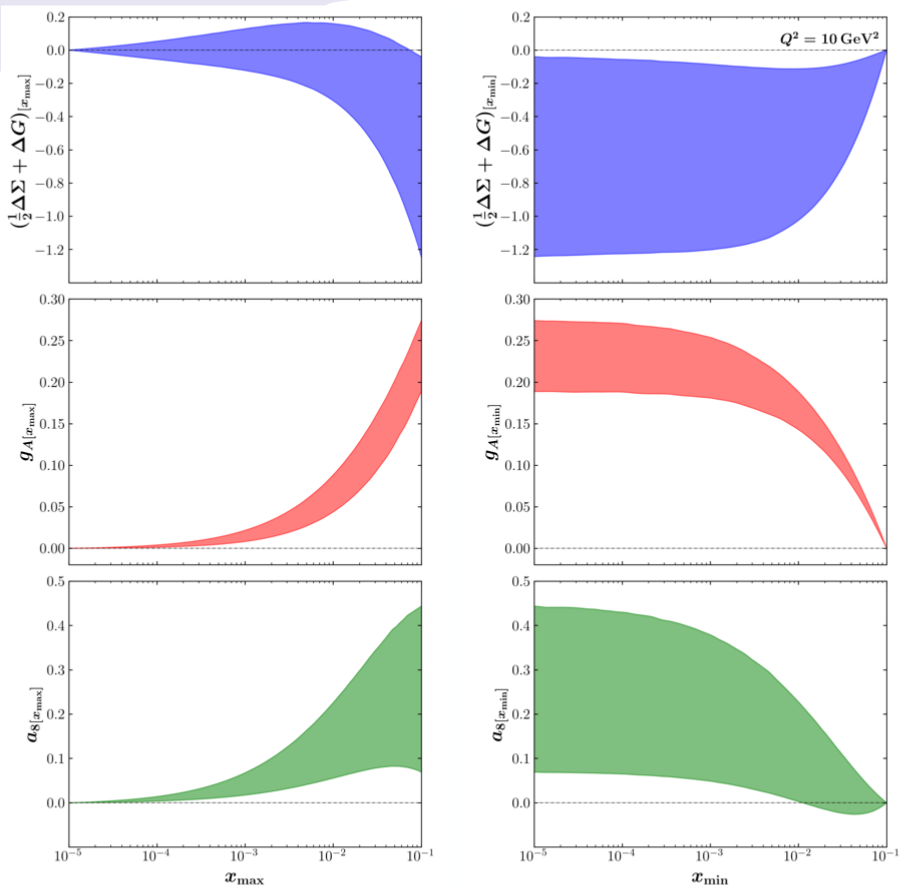

$$\left(\frac{1}{2}\Delta\Sigma + \Delta G\right)_{[x_{\min}]}(Q^2) \equiv \int_{x_{\min}}^{x_0} dx \left(\frac{1}{2}\Delta\Sigma + \Delta G\right)(x, Q^2)\,,$$

$$g_{A[x_{\min}]}(Q^2) \equiv \int_{x_{\min}}^{x_0} dx \left[\Delta u^+(x, Q^2) - \Delta d^+(x, Q^2)\right],$$

$$a_{8[x_{\min}]}(Q^2) \equiv \int_{x_{\min}}^{x_0} dx \left[\Delta u^+(x, Q^2) + \Delta d^+(x, Q^2) - 2\,\Delta s^+(x, Q^2)\right]$$

$$\left(\frac{1}{2}\Delta\Sigma + \Delta G\right)_{[x_{\max}]}(Q^2) \equiv \int_{10^{-5}}^{x_{\max}} dx \left(\frac{1}{2}\Delta\Sigma + \Delta G\right)(x, Q^2),$$

$$g_{A[x_{\max}]}(Q^2) \equiv \int_{10^{-5}}^{x_{\max}} dx \left[\Delta u^+(x, Q^2) - \Delta d^+(x, Q^2)\right],$$

$$a_{8[x_{\max}]}(Q^2) \equiv \int_{10^{-5}}^{x_{\max}} dx \left[\Delta u^+(x, Q^2) + \Delta d^+(x, Q^2) - 2\,\Delta s^+(x, Q^2)\right]$$

$$\int_{10^{-5}}^{0.1} \mathrm{d}x \left(\frac{1}{2}\Delta\Sigma + \Delta G\right)(x) = -0.64 \pm 0.60$$

Negative net spin at small x!

Potentially a lot of spin at small x. However, the uncertainties are large. Need a way to constrain the initial conditions. Stay tuned for inclusion of polarized p+p data from RHIC.

Particle production in polarized p+p collisions

YK, M. Li, 2403.06959 [hep-ph]

Gluon production at mid-rapidity

- We want to calculate gluon production cross section in polarized p+p collisions at mid-rapidity, where the gluon is small-x in both proton’s wave functions.

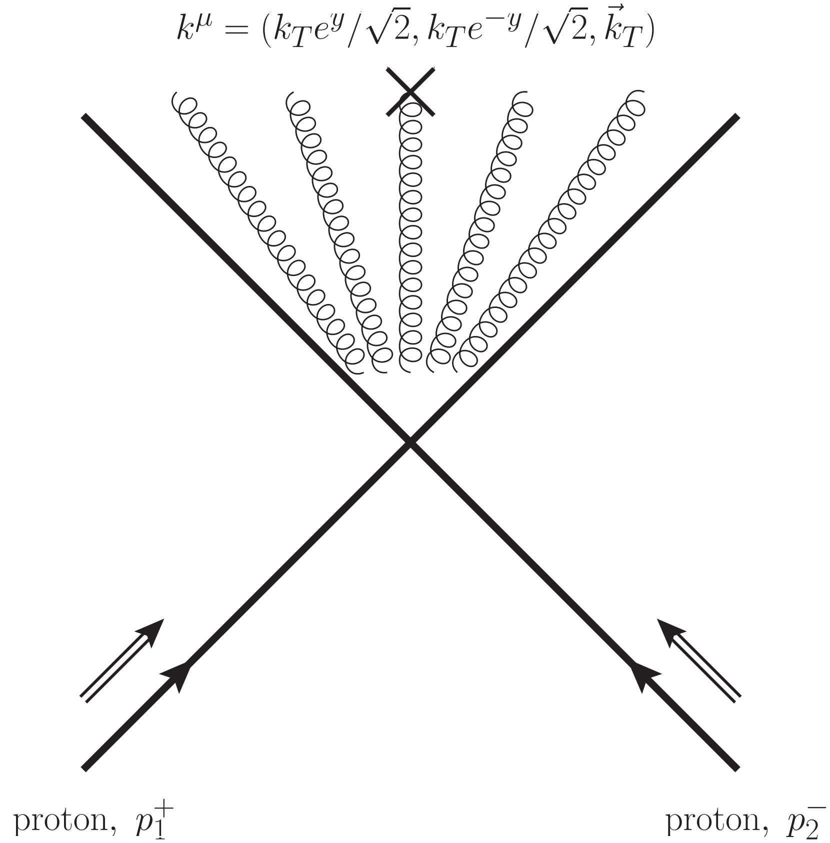

Gluon production in polarized p+p collisions

Working in the shock wave picture, we first need to sum up the following diagrams (emission inside shock wave is suppressed by a log):

The result is shown below, and is cross-checked against the existing lowest-order calculations.

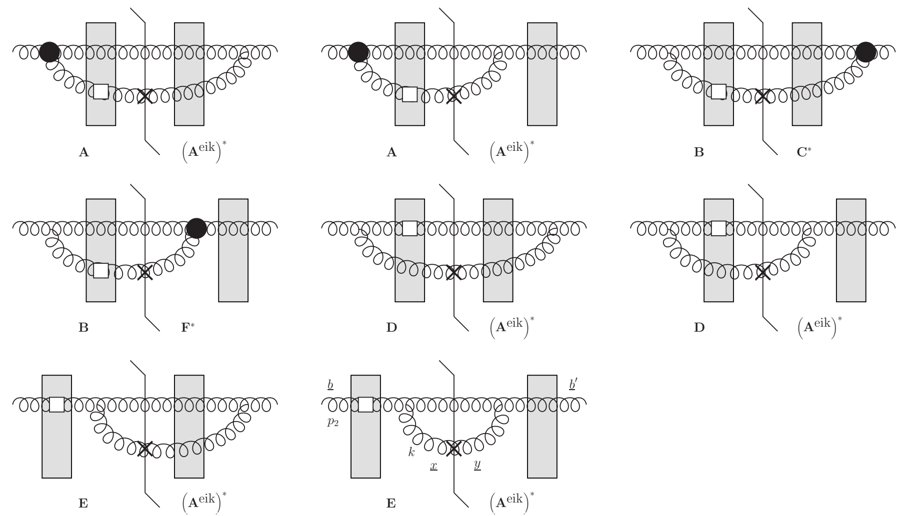

$$\frac{d\sigma(\lambda)}{d^2k_T\,dy} = \lambda\,\frac{\alpha_s}{\pi^4}\,\frac{1}{s}\,N_c \int d^2x\,d^2y\,d^2b\,e^{-i\underline{k}\cdot(\underline{x}-\underline{y})}\left\{\frac{\underline{x}-\underline{b}}{|\underline{x}-\underline{b}|^2}\cdot\frac{\underline{y}-\underline{b}}{|\underline{y}-\underline{b}|^2}\left[G^{\text{adj}}_{\underline{x},\underline{y}}(2k^-p_1^+) - G^{\text{adj}}_{\underline{x},\underline{b}}(2k^-p_1^+)\right.\right.$$
$$\left.\left. -\frac{1}{4}\left(G^{\text{adj}}_{\underline{b},\underline{y}}(2k^-p_1^+) + G^{\text{adj}}_{\underline{b},\underline{x}}(2k^-p_1^+) - 2\,G^{\text{adj}}_{\underline{b},\underline{b}'}(2k^-p_1^+)\right)\right] - 2i\,k^i\,\frac{\underline{x}-\underline{b}}{|\underline{x}-\underline{b}|^2}\times\frac{\underline{y}-\underline{b}}{|\underline{y}-\underline{b}|^2}\,G^{i\,\text{adj}}_{\underline{x},\underline{b}}(2k^-p_1^+)\right\}$$

Including small-x evolution

- We need to include small-x evolution on the projectile and target sides.
- This is simple on the target side, less so on the projectile side:

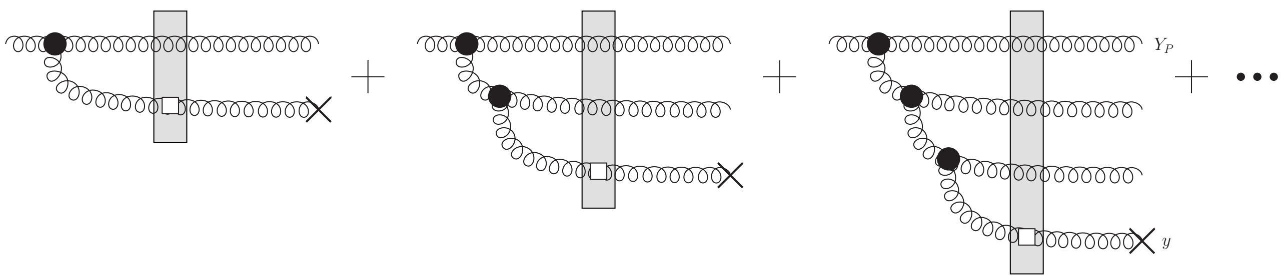

- We symmetrize the above expression with respect to target—projectile interchange, after which we can include the evolution on the projectile side as well.

Gluon production in polarized p+p collisions at mid-rapidity: the final result

- In the end we get the following expression for the cross section (at large N_c), where the dipole amplitudes Q and G_2 evolve via the above evolution equations (YK, M. Li, 2024):

$$\frac{d\sigma}{d^2k_T\,dy} = \frac{C_F}{\alpha_s\,\pi^4}\frac{1}{s\,k_T^2}\int d^2x\,e^{-i\underline{k}\cdot\underline{x}}$$
$$\times\,\begin{pmatrix}4\,Q_P & 2\,G_{2P}\end{pmatrix}(x_\perp^2,\sqrt{2}\,p_2^-\,k_T\,e^{-y})\begin{pmatrix}\frac{1}{4}\overleftarrow{\nabla}_\perp\cdot\vec{\nabla}_\perp & \overleftarrow{\nabla}_\perp^{\,2}+\overleftarrow{\nabla}_\perp\cdot\vec{\nabla}_\perp \\ \vec{\nabla}_\perp^2+\overleftarrow{\nabla}_\perp\cdot\vec{\nabla}_\perp & 0\end{pmatrix}\begin{pmatrix}4\,Q_T \\ 2\,G_{2T}\end{pmatrix}(x_\perp^2,\sqrt{2}\,p_1^+\,k_T\,e^{y}).$$

- Equivalently, in momentum space we obtain the following factorized expression in terms of TMDs ($\Delta H_{3L}^{\perp}$ is a twist-3 helicity-flip TMD):

$$\frac{d\sigma}{d^2k_T\,dy} = -\frac{32\pi^4\,\alpha_s}{N_c}\frac{1}{s\,k_T^2}\int\frac{d^2q}{(2\pi)^2}$$
$$\times\,\begin{pmatrix}\Delta H_{3L}^{\perp\,dip\,P} & g_{1L}^{G\,dip\,P}\end{pmatrix}\left(q_T^2,\frac{k_T}{\sqrt{2}\,p_2^-}\,e^{y}\right)\begin{pmatrix}\underline{q}\cdot(\underline{k}-\underline{q}) & \underline{q}\cdot\underline{k} \\ \underline{k}\cdot(\underline{k}-\underline{q}) & 0\end{pmatrix}\begin{pmatrix}\Delta H_{3L}^{\perp\,dip\,T} \\ g_{1L}^{G\,dip\,T}\end{pmatrix}\left((\underline{k}-\underline{q})^2,\frac{k_T}{\sqrt{2}\,p_1^+}\,e^{-y}\right)$$

Polarized p+p collisions: small-x phenomenology

- The above result can be applied to RHIC data (D. Adamiak, **N. Baldonado**, et al, 2503.21006 [hep-ph]):

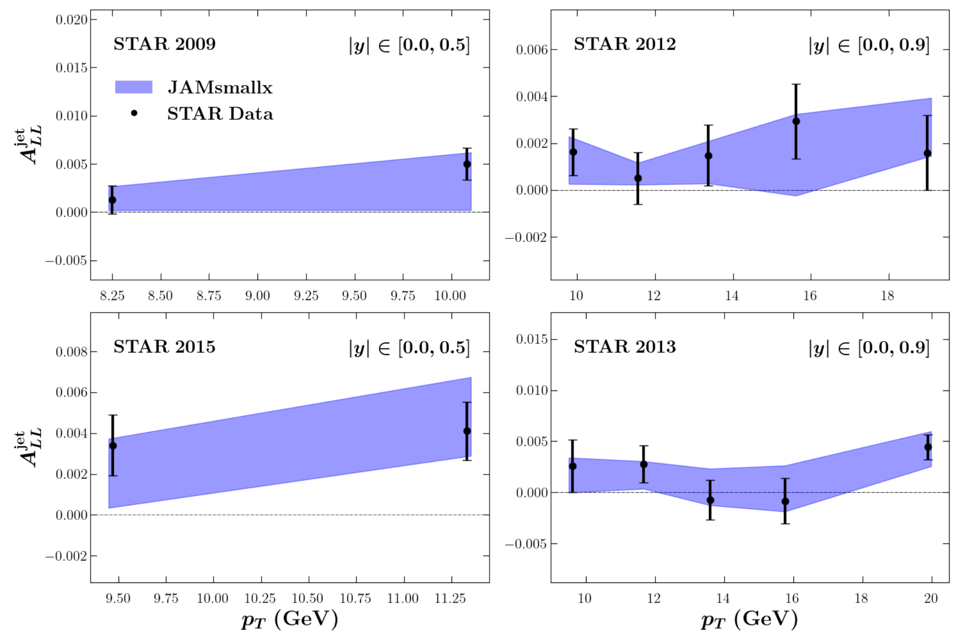

- Note that the calculation was for **gluons only**, quarks need to be included (in progress). Hence, comparison with the data is a proof-of-concept at this point.

- Only large-N_c evolution (+external quarks) is employed.

Longitudinal Spin: Small-x Evolution

- Small-x evolution can predict helicity distributions at small x.
- But: hard to fix initial conditions given the existing data (note: not all polarized p+p data has been analyzed yet).
- End result: also a spread of predictions for EIC.
- EIC will provide constraints:

- Plots are from JAMsmallx, D. Adamiak, **N. Baldonado**, et al, 2503.21006 [hep-ph]

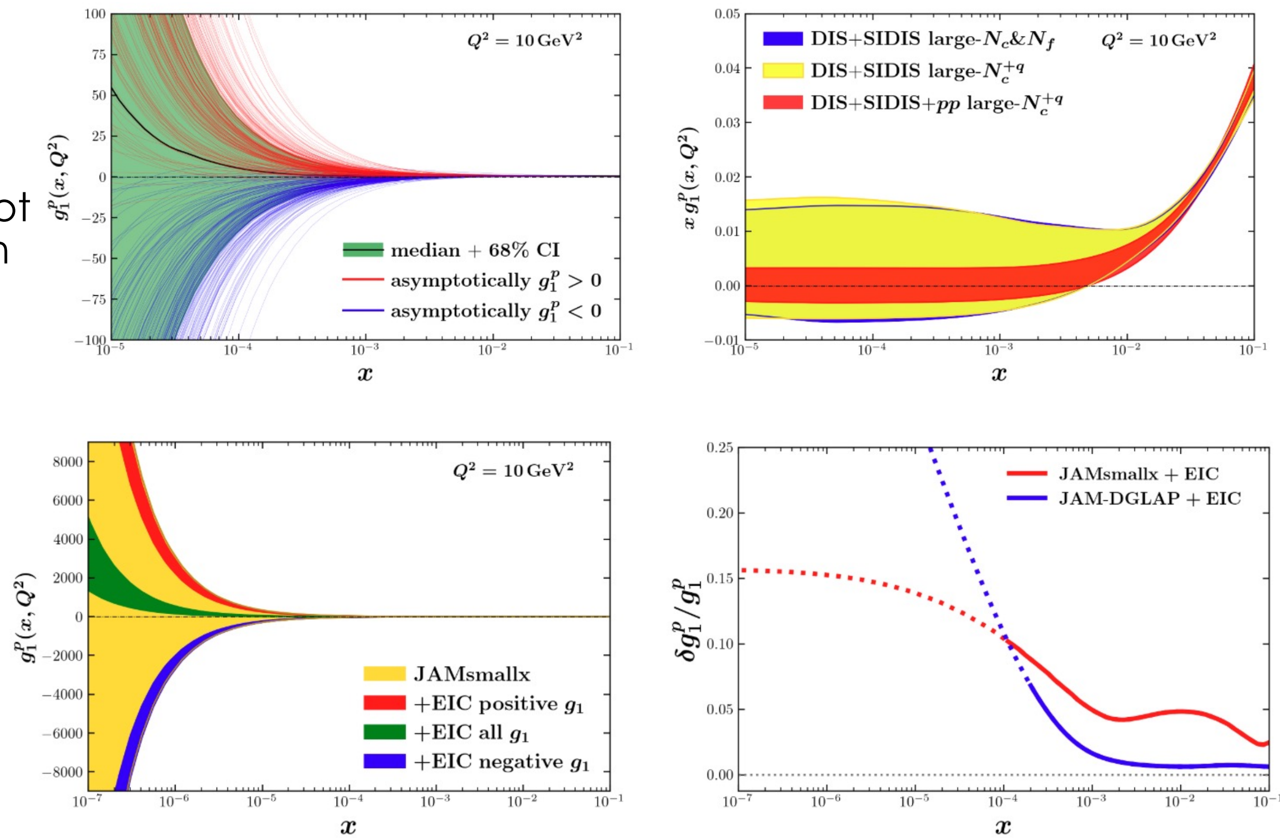

New constraints coming from polarized p+p data:

- Including more data constrains the initial conditions for the dipole amplitudes involved, resulting in more precise EIC predictions for the proton g_1 structure function and estimates of spin at low x:

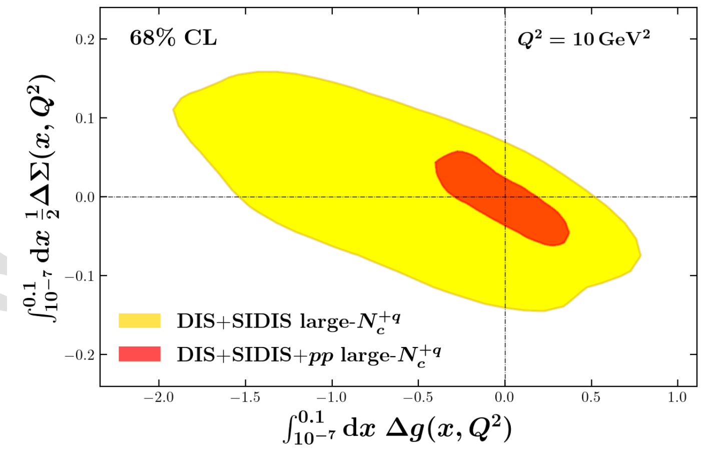

D. Adamiak, **N. Baldonado**, et al, 2503.21006 [hep-ph]

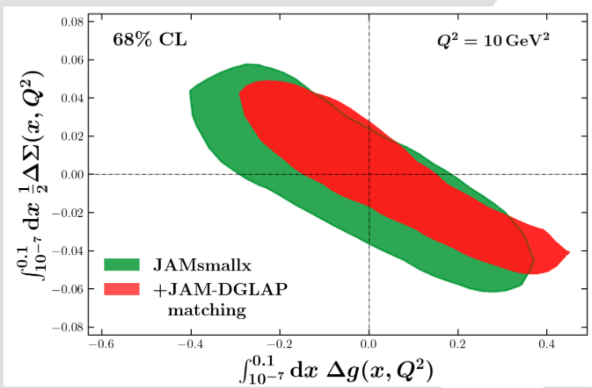

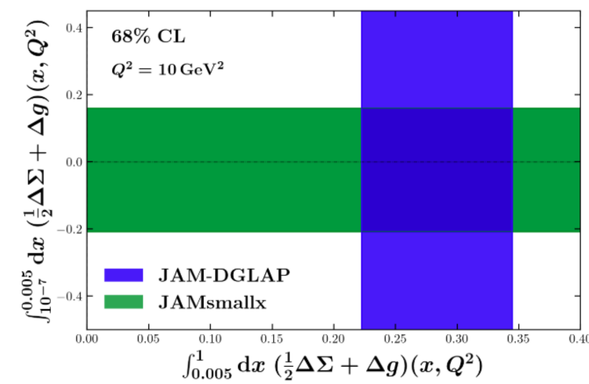

Quark and Gluon OAM at Small x and Large N_c

YK, B. Manley, 2310.18404 [hep-ph]; B. Manley, 2401.05508 [hep-ph];

YK, B. Manley, 2410.21260 [hep-ph].

OAM Distributions

- We begin by writing the (Jaffe-Manohar) quark and gluon OAM in terms of the Wigner distribution as

$$L_z = \int \frac{d^2 b_\perp \, db^- \, d^2 k_\perp \, dk^+}{(2\pi)^3} \, (\underline{b} \times \underline{k})_z \, W(k, b)$$

- After much algebra, we arrive at the quark and gluon OAM distributions at small x :

$$\Delta\Sigma(x, Q^2) = \frac{N_f}{\alpha_s \pi^2} \, \widetilde{Q} \left(x_{10}^2 = \frac{1}{Q^2}, s = \frac{Q^2}{x} \right),$$

$$\Delta G(x, Q^2) = \frac{2N_c}{\alpha_s \pi^2} \, G_2 \left(x_{10}^2 = \frac{1}{Q^2}, s = \frac{Q^2}{x} \right),$$

$$L_{q+\bar{q}}(x, Q^2) = -\frac{2\, N_f}{\alpha_s \pi^2} \, \widetilde{I} \left(x_{10}^2 = \frac{1}{Q^2}, s = \frac{Q^2}{x} \right),$$

$$L_G(x, Q^2) = -\frac{2\, N_c}{\alpha_s \pi^2} \left[2\, I_4 + 3\, I_5 \right] \left(x_{10}^2 = \frac{1}{Q^2}, s = \frac{Q^2}{x} \right)$$

OAM Distributions and Moment Amplitudes

$$L_{q+\bar{q}}(x, Q^2) = -\frac{2\,N_f}{\alpha_s \pi^2}\,\widetilde{I}\left(x_{10}^2 = \frac{1}{Q^2}, s = \frac{Q^2}{x}\right),$$

$$L_G(x, Q^2) = -\frac{2\,N_c}{\alpha_s \pi^2}\left[2\,I_4 + 3\,I_5\right]\left(x_{10}^2 = \frac{1}{Q^2}, s = \frac{Q^2}{x}\right)$$

- We now have the impact parameter **moments of dipole amplitudes/operators**:

$$\int d^2x_1\, x_1^m\, \widetilde{Q}_{10}(s) = x_{10}^m\, \widetilde{I}(x_{10}^2, s) + \epsilon^{mi} x_{10}^i\, \widetilde{J}(x_{10}^2, s)$$

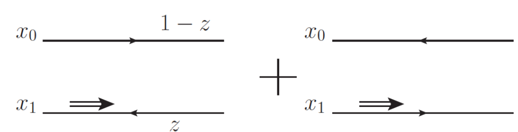

$$\int d^2x_1\, x_1^m\, Q_{10}(s) = x_{10}^m I_3(x_{10}^2, s) + \epsilon^{mj} x_{10}^j J_3(x_{10}^2, s),$$

$$\int d^2x_1\, x_1^m\, G_{10}^i(s) = \epsilon^{mi} x_{10}^2 I_4(x_{10}^2, s) + \epsilon^{mk} x_{10}^k x_{10}^i I_5(x_{10}^2, s) + \delta^{im} x_{10}^2 J_4(x_{10}^2, s) + x_{10}^i x_{10}^m J_5(x_{10}^2, s).$$

Evolution for Moment Dipole Amplitudes

Evolution equations for the moment amplitudes in DLA and at large N_c are derived in YK, B. Manley, 2310.18404 [hep-ph].

They can be solved numerically (same ref) and analytically (B. Manley, 2401.05508 [hep-ph])

$$\begin{pmatrix} I_3 \\ I_4 \\ I_5 \end{pmatrix}(x_{10}^2, zs) = \begin{pmatrix} I_3^{(0)} \\ I_4^{(0)} \\ I_5^{(0)} \end{pmatrix}(x_{10}^2, zs) + \frac{\alpha_s N_c}{4\pi} \int\limits_{\frac{1}{sx_{10}^2}}^{z} \frac{dz'}{z'} \int\limits_{\frac{1}{z's}}^{x_{10}^2} \frac{dx_{21}^2}{x_{21}^2} \begin{pmatrix} 2\,\Gamma_3 - 4\,\Gamma_4 + 2\,\Gamma_5 - 2\,\Gamma_2 \\ 0 \\ 0 \end{pmatrix}(x_{10}^2, x_{21}^2, z's)$$

$$+ \frac{\alpha_s N_c}{4\pi} \int\limits_{\frac{\Lambda^2}{s}}^{z} \frac{dz'}{z'} \int\limits_{\max[x_{10}^2, \frac{1}{z's}]}^{\min[\frac{z}{z'}x_{10}^2, \frac{1}{\Lambda^2}]} \frac{dx_{21}^2}{x_{21}^2} \begin{pmatrix} 4 & -4 & 2 & -4 & -6 \\ 0 & 4 & 2 & -2 & -3 \\ -2 & 2 & -1 & 4 & 7 \end{pmatrix} \begin{pmatrix} I_3 \\ I_4 \\ I_5 \\ G \\ G_2 \end{pmatrix}(x_{21}^2, z's)$$

$$\begin{pmatrix} \Gamma_3 \\ \Gamma_4 \\ \Gamma_5 \end{pmatrix}(x_{10}^2, x_{21}^2, z's) = \begin{pmatrix} I_3^{(0)} \\ I_4^{(0)} \\ I_5^{(0)} \end{pmatrix}(x_{10}^2, z's)$$

$$+ \frac{\alpha_s N_c}{4\pi} \int\limits_{\frac{1}{sx_{10}^2}}^{z'} \frac{dz''}{z''} \int\limits_{\frac{1}{z''s}}^{\min[x_{10}^2, x_{21}^2 \frac{z'}{z''}]} \frac{dx_{32}^2}{x_{32}^2} \begin{pmatrix} 2\,\Gamma_3 - 4\,\Gamma_4 + 2\,\Gamma_5 - 2\,\Gamma_2 \\ 0 \\ 0 \end{pmatrix}(x_{10}^2, x_{32}^2, z''s)$$

$$+ \frac{\alpha_s N_c}{4\pi} \int\limits_{\frac{\Lambda^2}{s}}^{z'\frac{x_{21}^2}{x_{10}^2}} \frac{dz''}{z''} \int\limits_{\max[x_{10}^2, \frac{1}{z''s}]}^{\min[\frac{z'}{z''}x_{21}^2, \frac{1}{\Lambda^2}]} \frac{dx_{32}^2}{x_{32}^2} \begin{pmatrix} 4 & -4 & 2 & -4 & -6 \\ 0 & 4 & 2 & -2 & -3 \\ -2 & 2 & -1 & 4 & 7 \end{pmatrix} \begin{pmatrix} I_3 \\ I_4 \\ I_5 \\ G \\ G_2 \end{pmatrix}(x_{32}^2, z''s)$$

Small-x asymptotics of OAM distributions

- Solving the above evolution equations numerically, we arrive at

$$L_{q+\bar{q}}(x, Q^2) \sim L_G(x, Q^2) \sim \left(\frac{1}{x}\right)^{3.66\sqrt{\frac{\alpha_s N_c}{2\pi}}}$$

Consistent with Boussarie, Hatta, Yuan, 2019 (based on BER IREE from 1996) within the numerical precision

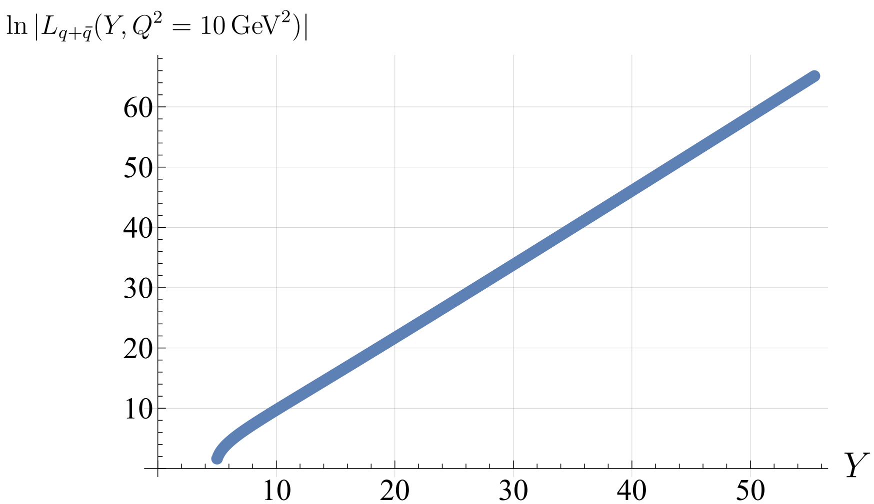

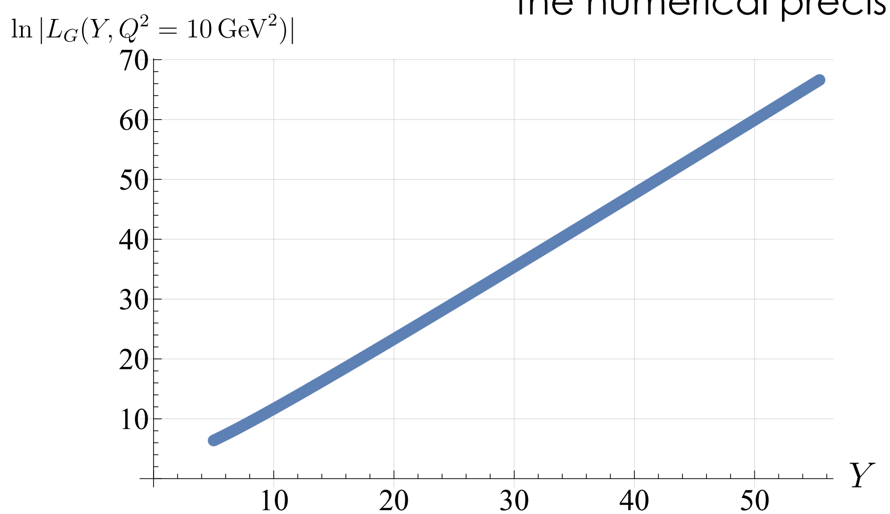

Two intercepts, again

- The evolution equations for moment dipole amplitudes have been solved analytically by B. Manley in 2401.05508 [hep-ph]. The solution was constructed using the double Laplace transform, similar to the solution for the impact-parameter integrated amplitudes.
- The resulting small-x OAM asymptotics at large N_c is the same as for helicity PDFs,

$$L_{q+\bar{q}}(x, Q^2) \sim L_G(x, Q^2) \sim \left(\frac{1}{x} \right)^{\alpha_h}$$

with the intercept

$$\alpha_h = \frac{4}{3^{1/3}} \sqrt{\mathrm{Re} \left[(-9 + i\,\sqrt{111})^{1/3} \right]} \sqrt{\frac{\alpha_s\, N_c}{2\pi}} \approx 3.661 \sqrt{\frac{\alpha_s\, N_c}{2\pi}}$$

- This slightly disagrees with the work of Boussarie, Hatta, and Yuan (2019), which resulted in the same intercept as BER:

$$\alpha_h = \sqrt{\frac{17 + \sqrt{97}}{2}} \sqrt{\frac{\alpha_s\, N_c}{2\pi}} \approx 3.664 \sqrt{\frac{\alpha_s\, N_c}{2\pi}}$$

OAM Distribution to hPDF Ratios

- Following Boussarie *et al* (2019), we consider the ratios of OAM distributions to helicity PDFs at small x.
- For these ratios, Boussarie *et al*, predict, inspired by the Wandzura-Wilczek approximation:

$$\frac{L_{q+\bar{q}}(x,Q^2)}{\Delta\Sigma(x,Q^2)} \approx -1 \qquad \frac{L_G(x,Q^2)}{\Delta G(x,Q^2)} \approx -2$$

$$\Delta\Sigma(x,Q^2)\Big|_{x\ll 1} \sim \Delta G(x,Q^2)\Big|_{x\ll 1} \sim \left(\frac{1}{x}\right)^{\alpha_h} \qquad L_{q+\bar{q}}(x,Q^2) \sim L_G(x,Q^2) \sim \left(\frac{1}{x}\right)^{\alpha_h}$$

- Pure WW approximation predicts:

$$\frac{L_{q+\bar{q}}(x,Q^2)}{\Delta\Sigma(x,Q^2)} = -\frac{1}{1+\alpha_h} \qquad \frac{L_G(x,Q^2)}{\Delta G(x,Q^2)} = -\frac{2}{1+\alpha_h}$$

OAM Distribution to hPDF Ratios

- Analytic solution from B. Manley, 2401.05508 [hep-ph], gives

$$t = \sqrt{\frac{\alpha_s N_c}{2\pi} \ln \frac{Q^2}{\Lambda^2}}$$

$$\alpha_s = 0.25 \qquad \Lambda = 1 \text{ GeV}$$

- Compares well with Boussarie *et al*:

$$\frac{L_{q+\bar{q}}(x,Q^2)}{\Delta\Sigma(x,Q^2)} \approx -1 \qquad \frac{L_G(x,Q^2)}{\Delta G(x,Q^2)} \approx -2$$

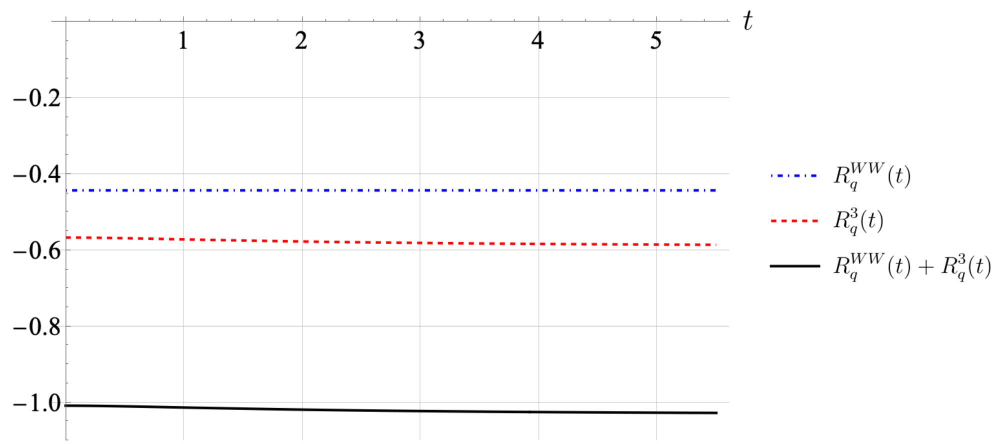

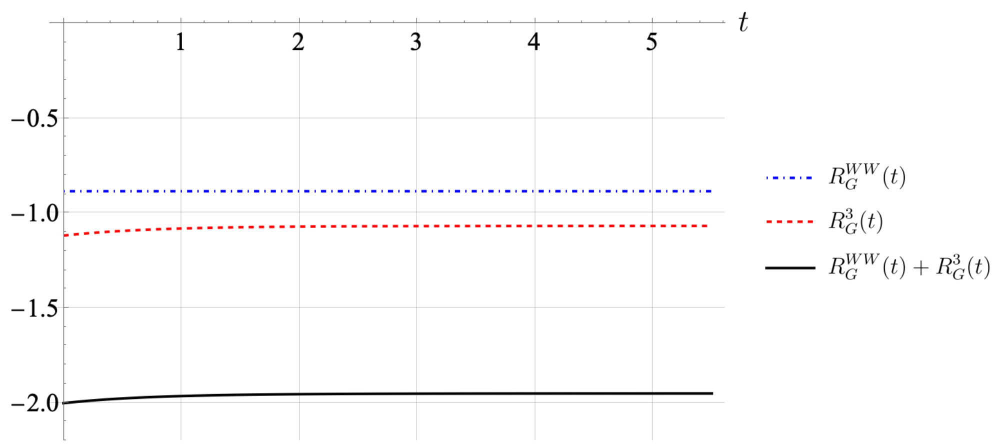

Elastic dijet production in e+p collisions

The process is similar to the one above, except now the proton remains intact.

One considers two observables, double spin asymmetry (DSA) and single spin asymmetry (SSA):

$$d\sigma^{DSA} = \frac{1}{4} \sum_{\sigma_e, S_L} \sigma_e \, S_L \, d\sigma(\sigma_e, S_L),$$

$$d\sigma^{SSA} = \frac{1}{4} \sum_{\sigma_e, S_L} S_L \, d\sigma(\sigma_e, S_L)$$

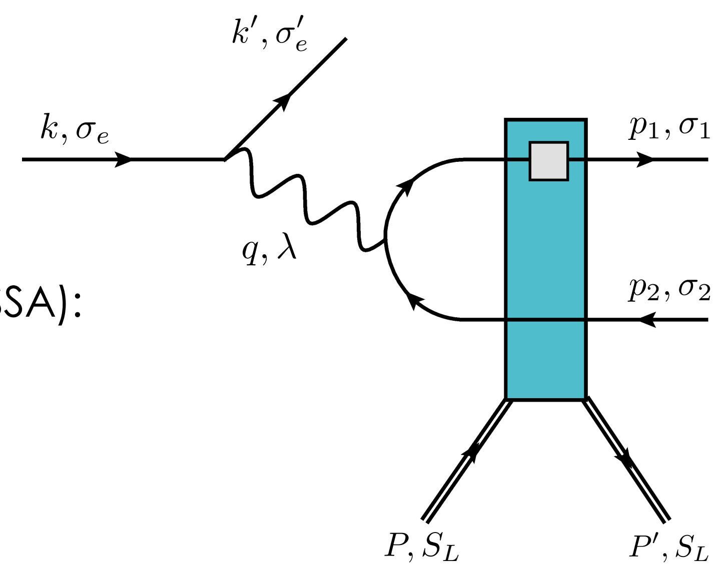

Hatta et al, 2016; S. Bhattacharya, R. Boussarie and Y. Hatta, 2022 & 2024; S. Bhattacharya, D. Zheng and J. Zhou, 2023; YK, B. Manley, 2410.21260 [hep-ph]

Measuring OAM distributions in elastic e+p collisions

- In the small-t limit (pT , Q >> $\Lambda_{QCD} \gg \Delta_\perp$ with $t = -\Delta_\perp^2$) the elastic dijet DSA measures moments of dipole amplitudes I_3, I_4, and I_5, thus **allowing (in principle) to measure OAM distributions!**
- Cf. Hatta et al, 2016; S. Bhattacharya, R. Boussarie and Y. Hatta, 2022 & 2024; S. Bhattacharya, D. Zheng and J. Zhou, 2023.
- Feasibility study in progress (G.Z. Becker, J. Borden, B. Manley, YK).

$$
\begin{aligned}
z(1-z)\,\frac{1}{2}\sum_{S_L,\lambda\pm1} S_L\,\lambda\,\frac{d\sigma^{\gamma^* p\to q\bar{q}p'}_{\text{symm. }\lambda\lambda}}{d^2p\,d^2\Delta\,dz} &= -\frac{2}{(2\pi)^5 z(1-z)s}\int d^2x_{12}\,d^2x_{1'2'}\,e^{-i\underline{p}\cdot(\underline{x}_{12}-\underline{x}_{1'2'})}\,N(x^2_{1'2'},s) \qquad (107\text{a})\\
\times\Bigg\{\Bigg[\bigg(1-2z+i\underline{\Delta}\cdot\underline{x}_{12}\,\left(z^2+(1-z)^2\right)&-\frac{i}{2}\,\underline{\Delta}\cdot\underline{x}_{1'2'}\,(1-2z)^2\bigg)\,Q(x^2_{12},s)-i\underline{\Delta}\cdot\underline{x}_{12}\,I_3(x^2_{12},s)\\
&-i\underline{\Delta}\times\underline{x}_{12}\,J_3(x^2_{12},s)\Bigg]\,\Phi^{[1]}_{\text{TT}}(\underline{x}_{12},\underline{x}_{1'2'},z)\\
+\Bigg[i(1-2z)\Big(\Delta^j\epsilon^{ji}x^2_{12}I_4(x^2_{12},s)&+\underline{\Delta}\times\underline{x}_{12}\,x^i_{12}I_5(x^2_{12},s)+\Delta^i\,x^2_{12}J_4(x^2_{12},s)+\underline{\Delta}\cdot\underline{x}_{12}\,x^i_{12}J_5(x^2_{12},s)\Big)\\
&-\left[1+i\,(1-2\,z)\,\underline{\Delta}\cdot\left(\underline{x}_{12}-\frac{\underline{x}_{1'2'}}{2}\right)\right]\left(\epsilon^{ik}x^k_{12}G_2(x^2_{12},s)+x^i_{12}G_1(x^2_{12},s)\right)\Bigg]\\
&\times\left(\partial^i_{\underline{1}}-ip^i\right)\Phi^{[2]}_{\text{TT}}(\underline{x}_{12},\underline{x}_{1'2'},z)\Bigg\}+\mathcal{O}(\Delta^2_\perp),
\end{aligned}
$$

$$
\begin{aligned}
z(1-z)\,\frac{1}{2}\sum_{S_L,\lambda=\pm1} S_L\left[e^{i\lambda\phi}\,\frac{d\sigma^{\gamma^* p\to q\bar{q}p'}_{\text{symm. }0\lambda}}{d^2p\,d^2\Delta\,dz}+\text{c.c.}\right] &= -\frac{2i\sqrt{2}}{2(2\pi)^5 z(1-z)s}\int d^2x_{12}\,d^2x_{1'2'}\,e^{-i\underline{p}\cdot(\underline{x}_{12}-\underline{x}_{1'2'})} \qquad (107\text{b})\\
\times N(x^2_{1'2'},s)\Bigg\{\Bigg[\bigg(1-2z+i\,\underline{\Delta}\cdot\underline{x}_{12}\,(z^2+(1-z)^2)&-\frac{i}{2}\underline{\Delta}\cdot\underline{x}_{1'2'}\,(1-2z)^2\bigg)\,Q(x^2_{12},s)-i\underline{\Delta}\cdot\underline{x}_{12}\,I_3(x^2_{12},s)\\
&-i\underline{\Delta}\times\underline{x}_{12}\,J_3(x^2_{12},s)\Bigg]\left[\frac{\hat{k}\cdot\underline{x}_{12}}{x_{12}}\Phi^{[1]}_{\text{LT}}(\underline{x}_{12},\underline{x}_{1'2'},z)-\frac{\hat{k}\cdot\underline{x}_{1'2'}}{x_{1'2'}}\Phi^{[1]}_{\text{LT}}(\underline{x}_{1'2'},\underline{x}_{12},z)\right]\\
+\Bigg[i(1-2z)\Big(\Delta^j\epsilon^{ji}\,x^2_{12}\,I_4(x^2_{12},s)&+\underline{\Delta}\times\underline{x}_{12}\,x^i_{12}\,I_5(x^2_{12},s)+\Delta^i\,x^2_{12}\,J_4(x^2_{12},s)+\underline{\Delta}\cdot\underline{x}_{12}\,x^i_{12}\,J_5(x^2_{12},s)\Big)\\
&-\left[1+i\,(1-2\,z)\,\underline{\Delta}\cdot\left(\underline{x}_{12}-\frac{\underline{x}_{1'2'}}{2}\right)\right]\left(\epsilon^{ik}x^k_{12}G_2(x^2_{12},s)+x^i_{12}G_1(x^2_{12},s)\right)\Bigg]\\
\times\left(\partial^i_{\underline{1}}-ip^i\right)&\left[\frac{\hat{k}\times\underline{x}_{12}}{x_{12}}\Phi^{[2]}_{\text{LT}}(\underline{x}_{12},\underline{x}_{1'2'},z)+\frac{\hat{k}\times\underline{x}_{1'2'}}{x_{1'2'}}\Phi^{[2]}_{\text{LT}}(\underline{x}_{1'2'},\underline{x}_{12},z)\right]\Bigg\}+\mathcal{O}(\Delta^2_\perp),
\end{aligned}
$$

YK, B. Manley, 2410.21260 [hep-ph]

OAM measurement with elastic dijets: feasibility study (very preliminary!)

Vertical axis – cos $\phi_{\Delta pT}$ harmonic in elastic dijets A_{LL}.

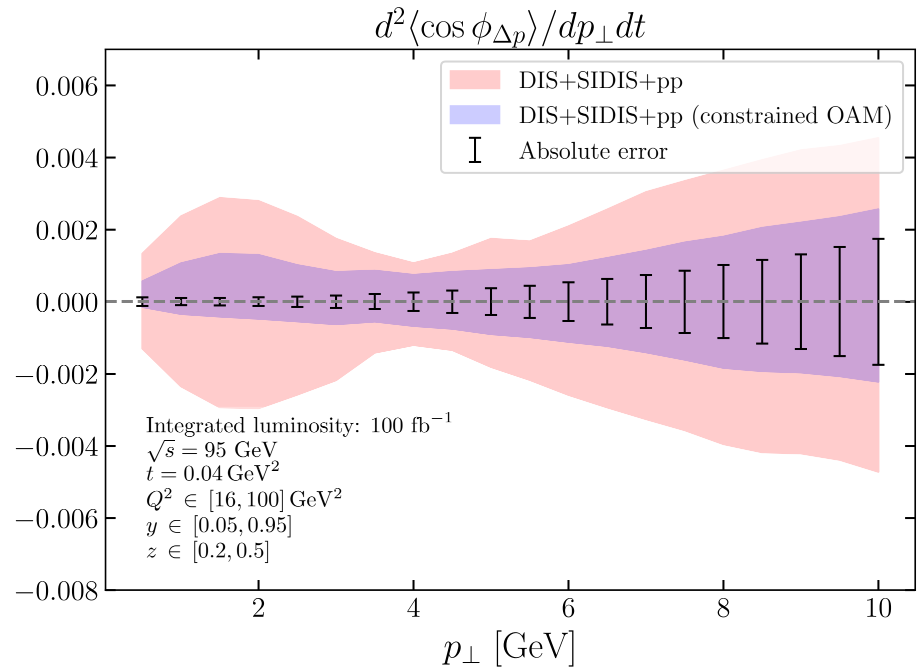

pT = jets b2b momentum
Δ = momentum transfer
assumed int. luminosity = 100 fb^{-1}

JAMsmallx (Brandon Manley) – **preliminary!**

Conclusions

We have constructed new evolution equations in x for the quark and gluon helicity distributions. We can now predict the x-dependence of helicity PDFs at small x.

These equations have now been solved at large-N_c yielding the small-x asymptotics of $\Delta\Sigma(x, Q^2)$ and $\Delta G(x, Q^2)$. The solution of the large-N_c&N_f equations will soon be on the arXiv as well.

First successful fit (JAMsmallx) of polarized world DIS+ SIDIS data for x<0.1 done using solely the small-x helicity evolution (KPS-CTT version of evolution). There is a clear possibility of a significant amount of proton spin to be found at small x. Some of the polarized p+p collisions data has recently been included in the fit as well.

Similar analysis has been carried out for the orbital angular momentum (OAM) distributions: small-x evolution equatons have been derived, small-x asymptotics for $L_q(x, Q^2)$ and $L_G(x, Q^2)$ have been obtained, and phenomenology (elastic dijets at EIC) is under way – one may be able to measure OAM at EIC!

This project is well on its way to resolve the (small-x part of the) proton spin puzzle, with the help of the EIC data.

Backup Slides

Resummation parameter

- BK equation resums powers of

$$\alpha_s \, N_c \, Y$$

- The Glauber-Mueller/McLerran-Venugopalan initial conditions resum powers of

$$\alpha_s^2 \, A^{1/3}$$

- Beyond the large-N_c limit: use the JIMWLK functional evolution equation (Iancu, Jalilian-Marian, Kovner, Leonidov, McLerran and Weigert, 1997-2002)

JIMWLK: derivation outline

A.H. Mueller, 2001

- Start by introducing a weight functional, $W_Y[\alpha]$. Here $\alpha = A^+$ is the gluon field of the target proton or nucleus. $\alpha(x^-, \vec{x}) \equiv A^+(x^+ = 0, x^-, \vec{x})$
- The functional is used to generate expectation values of gluon-field dependent operators in the target state:

$$\langle \hat{O}_\alpha \rangle_Y = \int \mathcal{D}\alpha \; \hat{O}_\alpha \, W_Y[\alpha]$$

- Imagine that we know small-x evolution for some operator O:

$$\partial_Y \, \langle \hat{O}_\alpha \rangle_Y = \langle \mathcal{K}_\alpha \otimes \hat{O}_\alpha \rangle_Y = \int \mathcal{D}\alpha \, \left[\mathcal{K}_\alpha \otimes \hat{O}_\alpha \right] \, W_Y[\alpha]$$

- On the other hand, we can differentiate the first equation above,

$$\partial_Y \, \langle \hat{O}_\alpha \rangle_Y = \int \mathcal{D}\alpha \; \hat{O}_\alpha \; \partial_Y \, W_Y[\alpha]$$

- Comparing the last two equations and integrating by parts in the second to last equation, we will arrive at and equation for the weight functional $W_Y[\alpha]$.

Quark Helicity Distribution at Small x

- One can show that the quark helicity PDF (ΔΣ) at small-x can be expressed in terms of the polarized dipole amplitude:

$$\Delta\Sigma(x, Q^2) \sim G(r_{10}^2, \beta)$$

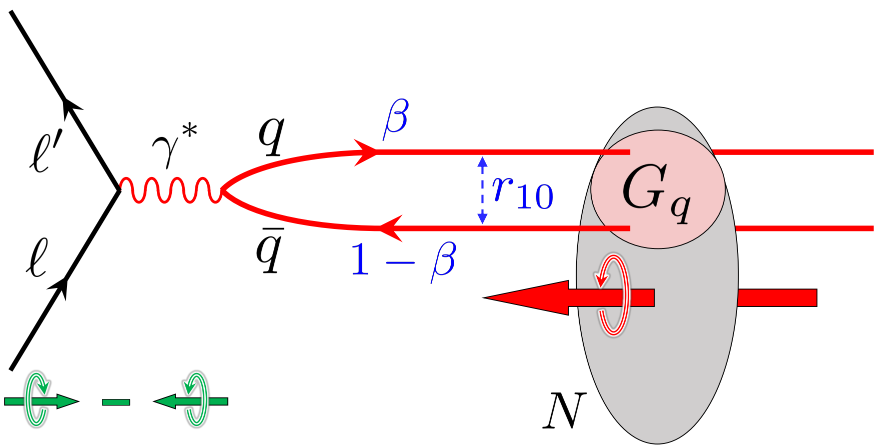

β = longitudinal momentum fraction (aka z);
r_{10} = (transverse) dipole size (aka x_{10})

$$\Delta\Sigma \equiv \Delta u + \Delta\bar{u} + \Delta d + \Delta\bar{d} + \Delta s + \Delta\bar{s}$$

Evolution for Polarized Quark Dipole

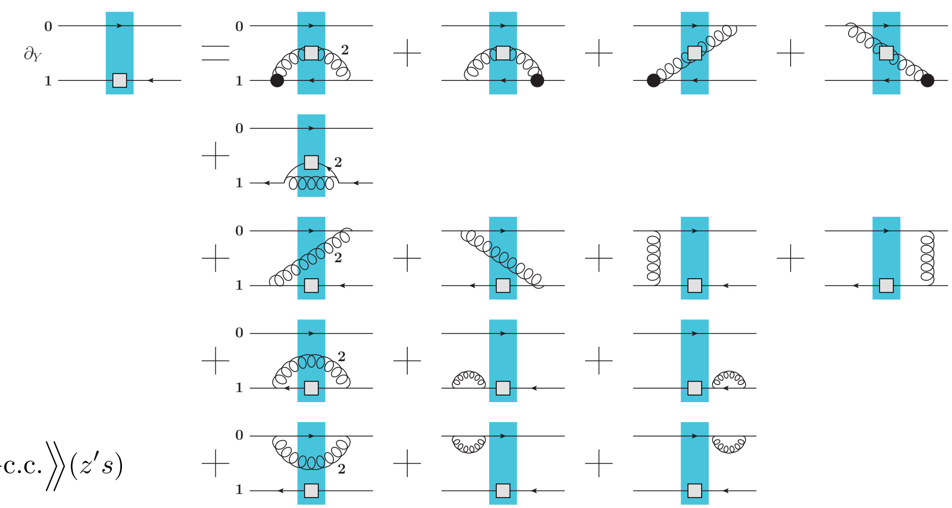

$$\langle\langle \ldots \rangle\rangle = z\, s\, \langle \ldots \rangle$$

$$\frac{1}{2N_c}\left\langle\!\!\left\langle \mathrm{tr}\left[V_{\underline{0}}\, V_{\underline{1}}^{\mathrm{pol}[1]\,\dagger}\right] + \mathrm{c.c.}\right\rangle\!\!\right\rangle(zs) = \frac{1}{2N_c}\left\langle\!\!\left\langle \mathrm{tr}\left[V_{\underline{0}}\, V_{\underline{1}}^{\mathrm{pol}[1]\,\dagger}\right] + \mathrm{c.c.}\right\rangle\!\!\right\rangle_0(zs)$$

$$+\frac{\alpha_s\, N_c}{2\pi^2}\int\limits_{\frac{\Lambda^2}{s}}^{z}\frac{dz'}{z'}\int d^2x_2\left\{\left[\frac{1}{x_{21}^2} - \frac{\underline{x}_{21}}{x_{21}^2}\cdot\frac{\underline{x}_{20}}{x_{20}^2}\right]\frac{1}{N_c^2}\left\langle\!\!\left\langle \mathrm{tr}\left[t^b V_{\underline{0}} t^a V_{\underline{1}}^{\dagger}\right]\left(U_{\underline{2}}^{\mathrm{pol}[1]}\right)^{ba} + \mathrm{c.c.}\right\rangle\!\!\right\rangle(z's)\right.$$

$$\left.+\left[2\frac{\epsilon^{ij}\, x_{21}^j}{x_{21}^4} - \frac{\epsilon^{ij}\,(x_{20}^j + x_{21}^j)}{x_{20}^2\, x_{21}^2} - \frac{2\,\underline{x}_{20}\times\underline{x}_{21}}{x_{20}^2\, x_{21}^2}\left(\frac{x_{21}^i}{x_{21}^2} - \frac{x_{20}^i}{x_{20}^2}\right)\right]\frac{1}{N_c^2}\left\langle\!\!\left\langle \mathrm{tr}\left[t^b V_{\underline{0}} t^a V_{\underline{1}}^{\dagger}\right]\left(U_{\underline{2}}^{i\,\mathrm{G}[2]}\right)^{ba}\right\rangle\!\!\right\rangle(z's)\right\}$$

$$+\frac{\alpha_s N_c}{4\pi^2}\int\limits_{\frac{\Lambda^2}{s}}^{z}\frac{dz'}{z'}\int\frac{d^2x_2}{x_{21}^2}\left\{\frac{1}{N_c^2}\left\langle\!\!\left\langle \mathrm{tr}\left[t^b\, V_{\underline{0}}\, t^a\, V_{\underline{2}}^{\mathrm{pol}[1]\,\dagger}\right]\, U_{\underline{1}}^{ba}\right\rangle\!\!\right\rangle(z's) + 2\,\frac{\epsilon^{ij}\,\underline{x}_{21}^j}{x_{21}^2}\,\frac{1}{N_c^2}\left\langle\!\!\left\langle \mathrm{tr}\left[t^b\, V_{\underline{0}}\, t^a\, V_{\underline{2}}^{i\,\mathrm{G}[2]\,\dagger}\right]\, U_{\underline{1}}^{ba}\right\rangle\!\!\right\rangle(z's)\right\}$$

$$+\frac{\alpha_s\, N_c}{2\pi^2}\int\limits_{\frac{\Lambda^2}{s}}^{z}\frac{dz'}{z'}\int d^2x_2\,\frac{x_{10}^2}{x_{21}^2\, x_{20}^2}\left\{\frac{1}{N_c^2}\left\langle\!\!\left\langle \mathrm{tr}\left[t^b\, V_{\underline{0}}\, t^a\, V_{\underline{1}}^{\mathrm{pol}[1]\,\dagger}\right]\, U_{\underline{2}}^{ba}\right\rangle\!\!\right\rangle(z's) - \frac{C_F}{N_c^2}\left\langle\!\!\left\langle \mathrm{tr}\left[V_{\underline{0}}\, V_{\underline{1}}^{\mathrm{pol}[1]\,\dagger}\right]\right\rangle\!\!\right\rangle(z's)\right\} + \mathrm{c.c.}$$

Equation does not close!